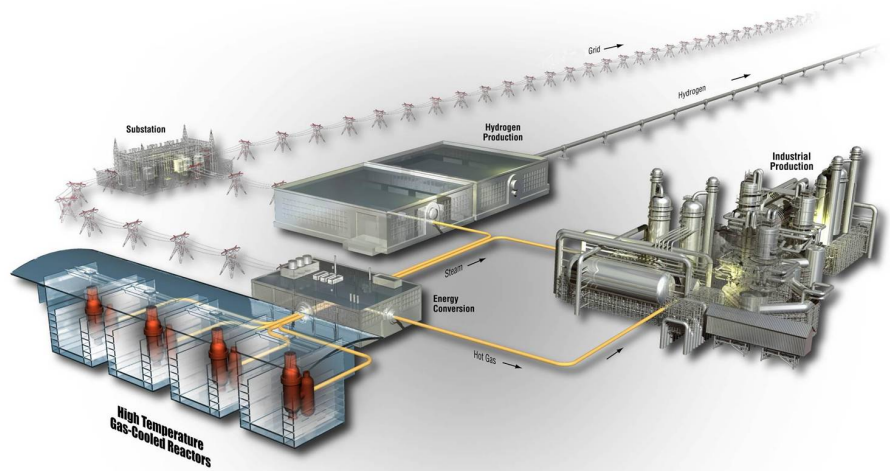


PEBBED Uncertainty and Sensitivity Analysis of the CRP-5 PBMR DLOFC Transient Benchmark with the SUSA Code

Gerhard Strydom

January 2011

The INL is a
U.S. Department of Energy
National Laboratory
operated by
Battelle Energy Alliance



DISCLAIMER

This information was prepared as an account of work sponsored by an agency of the U.S. Government. Neither the U.S. Government nor any agency thereof, nor any of their employees, makes any warranty, expressed or implied, or assumes any legal liability or responsibility for the accuracy, completeness, or usefulness, of any information, apparatus, product, or process disclosed, or represents that its use would not infringe privately owned rights. References herein to any specific commercial product, process, or service by trade name, trade mark, manufacturer, or otherwise, does not necessarily constitute or imply its endorsement, recommendation, or favoring by the U.S. Government or any agency thereof. The views and opinions of authors expressed herein do not necessarily state or reflect those of the U.S. Government or any agency thereof.

PEBBED Uncertainty and Sensitivity Analysis of the CRP-5 PBMR DLOFC Transient Benchmark with the SUSA Code

Gerhard Strydom

January 2011

**Idaho National Laboratory
Next Generation Nuclear Plant Project
Idaho Falls, Idaho 83415**

**Prepared for the
U.S. Department of Energy
Office of Nuclear Energy
Under DOE Idaho Operations Office
Contract DE-AC07-05ID14517**

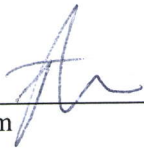
Next Generation Nuclear Plant Project

**PEBBED Uncertainty and Sensitivity Analysis of the
CRP-5 PBMR DLOFC Transient Benchmark with the
SUSA Code**

INL/EXT-10-20531

January 2011

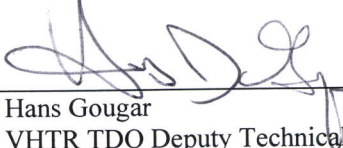
Approved by:



Gerhard Strydom
Author

01/04/2011

Date



Hans Gougar
VHTR TDO Deputy Technical Director

01/04/2011

Date



Diane V. Croson
VHTR TDO Deputy Director

1/4/11

Date

ABSTRACT

The need for a defensible and systematic uncertainty and sensitivity approach that conforms to the code scaling, applicability, and uncertainty (CSAU) process, and that could be used for a wide variety of software codes, was defined in 2008. The Gesellschaft für Anlagen und Reaktorsicherheit (GRS) company of Germany has developed one type of CSAU approach that is particularly well suited for legacy coupled core analysis codes, and a trial version of their Software for Uncertainty and Sensitivity Analyses (SUSA) was acquired on May 12, 2010. This report summarized the results of the initial investigations performed with SUSA, utilizing a typical High Temperature Reactor benchmark (the International Atomic Energy Agency CRP-5 Pebble Bed Modular Reactor 400 MW Exercise 2) and the PEBBED-THERMIX suite of codes. The following steps were performed as part of the uncertainty and sensitivity analysis:

1. Eight PEBBED-THERMIX model input parameters were selected for inclusion in the uncertainty study: total reactor power, inlet gas temperature, decay heat, and the specific heat capability and thermal conductivity of the fuel, pebble bed, and reflector graphite.
2. The input parameters variations and probability density functions were specified, and a total of 800 PEBBED-THERMIX model calculations were performed, divided into four sets of 100 and two sets of 200 steady-state and depressurized loss of forced cooling (DLOFC) transient calculations each.
3. The steady-state and DLOFC maximum fuel temperature and the daily pebble fuel load rate data were supplied to SUSA as model output parameters of interest. The six data sets were statistically analyzed to determine the 5% and 95% percentile values for each of the three output parameters with a 95% confidence level, and typical statistical indicators were also generated (e.g., Kendall, Pearson, and Spearman coefficients).
4. A SUSA sensitivity study was performed to obtain correlation data between the input and output parameters, and to identify the primary contributors to the output data uncertainties.

It was found that the uncertainties in the decay heat, pebble bed, and reflector thermal conductivities were responsible for the bulk of the propagated uncertainty in the DLOFC maximum fuel temperature. It was also determined that the two standard deviation (2σ) uncertainty on the maximum fuel temperature was between $\pm 58^\circ\text{C}$ (3.6%) and $\pm 76^\circ\text{C}$ (4.7%) on a mean value of 1604°C . These values mostly depended on the selection of the distributions types, and not on the number of model calculations above the required Wilks' criteria.

CONTENTS

ABSTRACT.....	v
ACRONYMS.....	xi
1. INTRODUCTION.....	1
1.1 Overview of General Uncertainty Analysis in Coupled Code Simulations	1
1.2 Uncertainty Propagation Methodology	2
2. FEATURES OF THE GRS STATISTICAL UNCERTAINTY METHOD AND SUSAS.....	6
3. SUSAS TEST CASE: PEBBED-THERMIX DLOFC	8
3.1 Code, Model, and FOM Selection.....	9
3.2 Input Parameters, Distribution Types and Variations	9
3.3 SUSAS Statistical Input Data Generation	11
3.4 PEBBED-THERMIX Calculation Results.....	17
3.5 SUSAS Uncertainty Analysis.....	23
3.6 Sensitivity Analysis.....	27
3.6.1 Parametric Variation Study Results	27
3.6.2 SUSAS Sensitivity Study Results	28
4. CONCLUSIONS	33
5. REFERENCES	34
APPENDIX A Summary of Changes Made to the PEBBED and THERMIX Codes for SUSAS Implementation.....	36

FIGURES

Figure 1. Illustration of the CSAU methodology.....	3
Figure 2. Example of the GRS methodology applied to the PEBBED CRP-5 PBMR 400 Exercise 2 benchmark calculation.	9
Figure 3. SUSAS input parameters distribution information entry screen.....	11
Figure 4. SUSAS entry screen for “Total Power” distribution information.....	12
Figure 5. PDF for the total power input parameter.	12
Figure 6. PDFs for the specific heat and thermal conductivity correlation input parameters.....	13
Figure 7. Cumulative density function for the total power.	13
Figure 8. SUSAS random generator GUI dialogue.....	15
Figure 9. Sampled values of the total power (MW) for the 200 LHS Normal set.	16
Figure 10. Sampled values of the reflector conductivity multiplication factor for the 200 LHS Normal set.....	16

Figure 11. DLOFC maximum fuel temperature vs. time for the first 30 cases of the 100 SRS Uniform set.....	18
Figure 12. DLOFC maximum fuel temperature vs. time for the first 30 cases of the 100 LHS Normal set.....	18
Figure 13. DLOFC maximum fuel temperature vs. time for the first 30 cases of the 200 LHS Normal set.....	19
Figure 14. DLOFC maximum fuel temperature vs. time for the first 30 cases of the 200 LHS Normal set: detail of the peak temperature turning points.....	19
Figure 15. DLOFC maximum fuel temperature vs. time for all 200 cases of the 200 LHS Normal set.....	20
Figure 16. DLOFC maximum fuel temperature vs. time for eight cases of the 100 LHS Normal set.....	21
Figure 17. Maximum DLOFC fuel temperature of the 200 LHS Normal set at 50 hours.	21
Figure 18. Maximum steady-state fuel temperature of the 200 LHS Normal set at 0 hours.	22
Figure 19. Daily fuel loading rate of the 200 LHS Normal set.....	22
Figure 20. PDF and fitted normal distribution results for the 100 LHS Normal set: K-S level of significance = 0.9919.....	23
Figure 21. PDF and fitted Weibull distribution results for the 100 LHS Normal set: K-S level of significance = 0.2231.....	24
Figure 22. PDF and fitted uniform distribution results for the 100 LHS Normal set: K-S Level of Significance = 0.0026.....	24
Figure 23. Time dependent minima, maxima, means and 5/95 percentiles for the 200 LHS Normal set maximum fuel temperature.	27
Figure 24. Kendall rank correlation coefficients (peak fuel temperature) for the 100 LHS Uniform set.....	29
Figure 25. Kendall rank correlation coefficients (peak fuel temperature) for the 200 LHS Normal set.....	29
Figure 26. Empirical correlation ratios (peak fuel temperature) for the 100 LHS Uniform set.....	30
Figure 27. Empirical correlation ratios (peak fuel temperature) for the 200 LHS Normal set.	30
Figure 28. Empirical correlation ratios (pebble load rate) for the 200 LHS Normal set.....	31
Figure 29. Empirical correlation ratios (peak fuel temperature) variations vs. time for the 200 LHS Normal set.	31

TABLES

Table 1. Comparison between statistical and deterministic uncertainty assessment methodologies.	5
Table 2. Test platform and SUSAs code details.	8
Table 3. PEBBED CRP-5 DLOFC uncertainty study input parameters.	10
Table 4. PEBBED-THERMIX CRP-5 DLOFC uncertainty study cases.....	14
Table 5. PEBBED-THERMIX input data for the first 10 model runs of the 200 LHS Normal set.....	15

Table 6. Lilliefors test results for the 200 LHS Normal set.	25
Table 7: K-S test results for the 200 LHS Normal set.	25
Table 8: PEBBED CRP-5 DLOFC uncertainty study results.	25
Table 9: Parametric variation study results.	28

ACRONYMS

CSAU	Code Scaling, Applicability, and Uncertainty
DLOFC	depressurized loss of forced cooling
FOM	Figure of Merit
GRS	Gesellschaft für Anlagen und Reaktorsicherheit
GUI	graphical user interface
IAEA	International Atomic Energy Agency
INL	Idaho national Laboratory
LHS	Latin hypercube sampling
PBMR	pebble bed modular reactor
PDF	probability density function
PIRT	Phenomena Information and Ranking Table
RIT	reactor inlet (gas) temperature
SRS	simple random sampling
SUSA	Software for Uncertainty and Sensitivity Analyses
TDO	Technology Development Office
TINTE	Time Dependent Neutronics and Temperatures
VHTR	Very High Temperature Reactor
UAM	Uncertainty in Analysis Modeling

1. INTRODUCTION

Title 10 Part 50 (10 CFR 50.46) of the United States Code of Federal Regulations first allowed “Best Estimate” calculations rather than conservative code models of safety parameters in nuclear power plants in the 1980s, stipulating, however, that uncertainties be identified and quantified (Anon 1996). Since then, various approaches to uncertainty analysis have been developed, accepted, and used for some light water reactor severe accidents. The simulation of the equilibrium neutronic and thermal-hydraulic characteristics of a reactor necessarily requires the application of a coupled-code system, such as PEBBED (Gougar 2010a) or CYNOD (Hiruta 2008), to capture all the relevant physics. Propagating the uncertainty in various input parameters, models, and assumptions through to the output figures of merit (for example fuel temperature) is a process that is still under development in many countries.

1.1 Overview of General Uncertainty Analysis in Coupled Code Simulations

In general, code uncertainty refers to uncertainty in the ability of a computer software product, coupled with a specific model, to accurately describe the actual physical system of interest. The computer model is an integration of the mathematical model, the numerical techniques used to solve those equations, and the representation of the physical model by the input geometry and material specifications. Each element contributes to the total uncertainty in the output parameter of interest, usually referred to as the Figure of Merit (FOM) in nuclear safety studies.

The mathematical model consists of one or more governing equations that describe the balance between the creation, destruction, and flow of some quantity of interest (e.g., heat, coolant mass, or neutron flux) within a homogeneous control volume. It also consists of one or more subgrid equations that relate these gross phenomena to more complex physics that are neglected at the scale of the homogeneous control volume (e.g. neutron streaming between pebbles, heat conduction from the kernels to the pebble surface, etc.). The uncertainty associated with the mathematical model can be estimated by comparing the results with those generated using a different model that captures these phenomena more accurately or uses different governing equations or subgrid relations.

A further complication is that very few computer codes solve the analytic form of its governing equations. Instead, the differential operators in these equations are expanded as a truncated series and cast as a set of difference equations solved over a discrete mesh. If the equations are well posed, the solution is unique and refining the mesh reduces the error between the solutions of the discretized equation and the original differential equation. Unfortunately, unlimited mesh refinement is not possible and one must tolerate some truncation error. Furthermore, in many complex fluid system simulation codes, the combination of governing equations and subgrid correlations yields ill-posed systems of differential equations that do not converge to the analytical solution upon refinement of the mesh. These errors can be shown to be minimal in codes like PEBBED and CYNOD, provided that the physical system is within the original range of applicability of the code. Nonetheless, in order to estimate the uncertainty introduced by the numerical approximations implemented in the code, direct comparisons to higher fidelity models can be performed.

Another important source of uncertainty is that the input model is a simplification of the actual physical geometry. For example, the distribution of pebbles in the core is neither regular nor uniform, but to model it as anything else is computationally prohibitive. Complex geometrical detail in some of the prismatic designs can likewise be very difficult, if not impossible, to model accurately. In such cases, high fidelity models of only the core features in question can be constructed with reasonable boundary conditions provided by the larger core or system model. The results, in terms of the desired FOM, can be compared with its lower fidelity counterparts with uncertainty values derived from the differences.

The fourth major source of input uncertainty is the material neutronic and thermophysical properties. For core analysis, these include thermal properties such as conductivity and heat capacity, fluid properties such as density and viscosity, and neutronic properties such as cross sections. Knowledge of these parameters for each material of interest may be limited in the range of conditions found in a new type of reactor. Such uncertainty can be reduced through material testing and measurement, but the amount of testing is often limited by cost and schedule constraints and must be propagated through the calculations. In some cases, the natural variability of a given parameter under even the best experimental conditions may be large enough to inject uncertainty that cannot be ignored. Finally, when modeling of an actual operating reactor is considered, it is well known that the operational conditions (power level, inlet temperature, measured mass flow rates) can also have associated uncertainty ranges.

(The sources of uncertainty discussed up to now are distinct from “human” errors in the code and model that usually arise from developer/user errors. These factors are usually addressed as part of the code development, calculation review, and quality assurance processes).

1.2 Uncertainty Propagation Methodology

Of the four types of uncertainty sources indicated here, the uncertainties in material properties can usually be addressed by relatively simple manipulation of the corresponding values in the input decks, and geometry simplifications can be benchmarked against higher fidelity codes (e.g., 2-D vs. 3-D effects). In contrast, variations in mathematical models and solver techniques are much more challenging, and in most cases not yet attempted in industry. Developments in uncertainty methodology are therefore currently focused on model and material input data uncertainties, and specifically on the propagation of uncertainties through coupled neutronic and thermal-fluid calculations. A recent example of a comprehensive thermal-fluid uncertainty propagation study is Phase 3 of the Organization for Economic Co-operation and Development/Nuclear Energy Agency BEMUSE program (De Crécy 2008), where 11 participants calculated uncertainty and sensitivity data for a large break loss of cooling accident. An even larger international uncertainty and sensitivity quantification effort is also underway as part of the OECD’s Uncertainty in Analysis Modeling (UAM) program, where nine consecutive uncertainty estimate phases cover all aspects of a coupled boiling water reactor calculation (Ivanov 2007). This series of benchmark calculations will start with the propagation of uncertainties during the generation of the multigroup cross-section libraries, up to the final loss of forced cooling accident analysis that require time dependent coupled neutronics, thermal fluids and system response modeling.

The need for a defensible and systematic uncertainty and sensitivity approach that conforms to the Nuclear Regulatory Commission’s Code Scaling, Applicability, and Uncertainty (CSAU) process, and that could be used for a wide variety of software codes, was defined in 2008 at Idaho National Laboratory’s (INL’s) Very High Temperature Reactor (VHTR) Technology Development Office. The GRS (Gesellschaft für Anlagen und Reaktorsicherheit) company of Germany has developed one type of CSAU approach that is particularly well suited for legacy coupled core analysis codes, and a trial version of their commercial software product SUSA (Software for Uncertainty and Sensitivity Analyses) (Langebusch 2005) was acquired on May 12, 2010. Development of SUSA’s predecessors started in the mid eighties, and the code has been used extensively in uncertainty and sensitivity calculations (e.g., recently GRS teams used SUSA for the BEMUSE and UAM benchmarks).

This report contains the results of the initial investigations performed with SUSA, utilizing the International Atomic Energy Agency (IAEA) CRP5 Pebble Bed Modular Reactor (PBMR) 400 MW benchmark (Reitsma 2010) model and the PEBBED-THERMIX suite of codes.

A detailed discussion of the CSAU methodology can be found in the literature (e.g., see Boyack 1990, and NUREG/CR-5249 1989). Figure 1 presents a diagram illustrating the CSAU methodology.

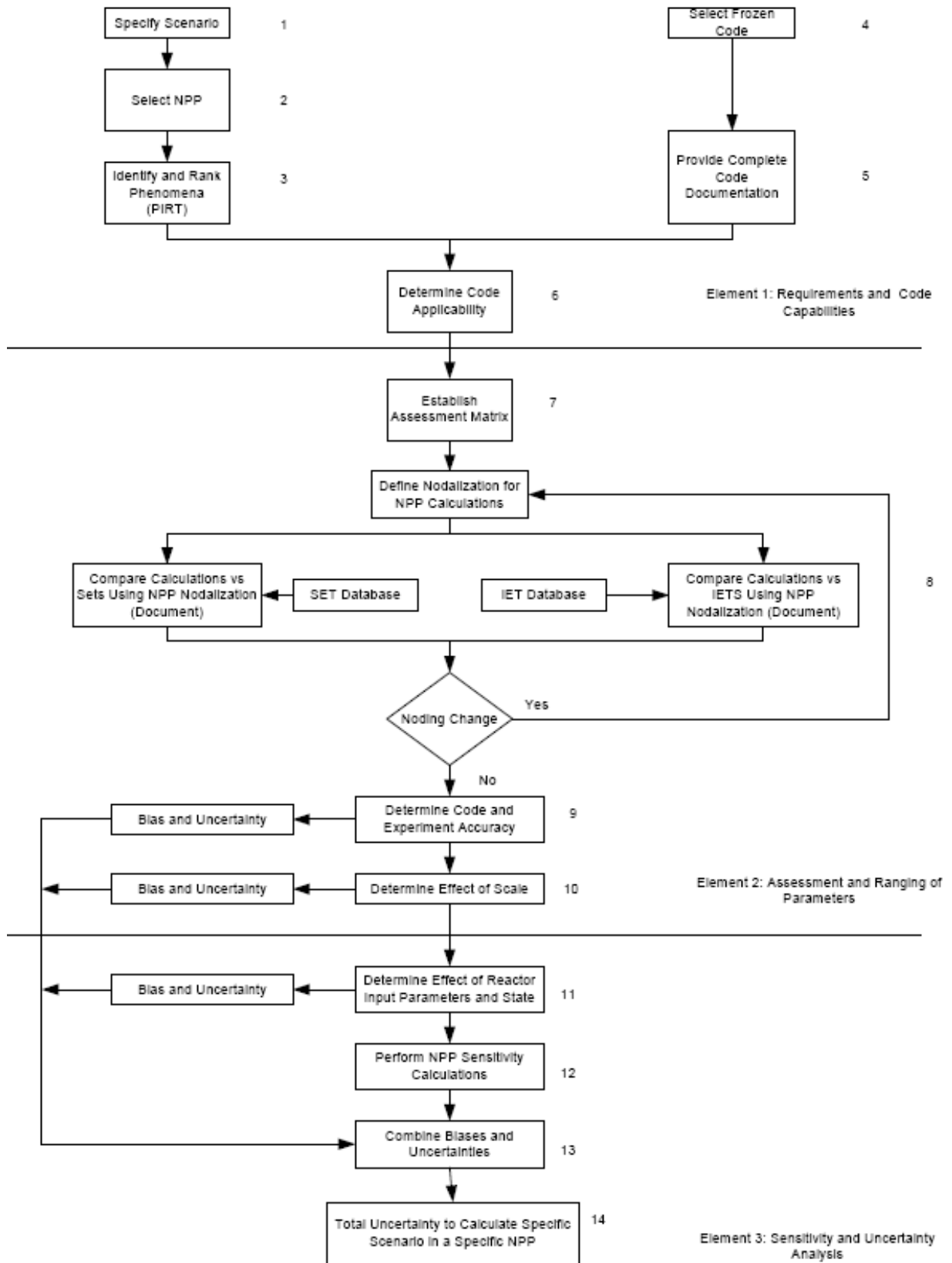


Figure 1. Illustration of the CSAU methodology.

Fourteen steps are incorporated into the three elements as indicated by the numbers on the figure. After specifying a scenario and nuclear power plant design for analysis (*Steps 1 and 2*), a Phenomena Identification and Ranking Table (PIRT) is generated by a panel of experts (*Step 3*) to identify important phenomena for subsequent evaluation. In the CSAU methodology, the PIRT is used to guide the uncertainty quantification. NUREG/CR-5249 (1989) identifies several techniques for accomplishing the ranking in a PIRT, including expert opinion, subjective decision-making methods, and scoping calculations. A PIRT was recently completed for the thermal fluid and neutronics phenomena of importance to the Next generation Nuclear Plant design (Ball et al. 2007), and the PEBBED-THERMIX codes typically include the modeling of most of these phenomena.

Steps 4 and 5 consist of selecting a documented computer code to be used for the analysis; the applicability of the code is evaluated in *Step 6*. This evaluation typically includes a review of the code capability to determine whether the code is suitable to be used for analyzing the transient of interest. The PEBBED-THERMIX methodology and solvers were evaluated to determine if the PBMR 400 MW CRP5 steady-state and depressurized loss of forced cooling (DLOFC) can be treated, and it was found that although THERMIX is not capable of time dependent convective heat transfer, the DLOFC can be adequately represented with only conduction and radiation heat transfer taken into account (this can be shown with code-to-code comparisons, e.g., comparing the PEBBED-TEHRMIX DLOFC results with the TINTE (Time Dependent Neutronics and Temperatures) code results, as reported in Strydom 2004). These first six steps are included in the Requirements and Capabilities Element.

Steps 7 to 10 are part of the Assessment and Ranging of Parameters Element. These steps are needed to quantify the effects of the individual contributors to uncertainty, and could include code limitations and scaling effects embedded in experimental data and code. Since the PBMR is not yet operational, only *Step 8* was performed for this study, i.e., a PBMR model was developed using a nodalization that is sufficiently fine to capture important phenomena and plant design characteristics without being too penalizing from a computer execution time perspective.

The remaining four steps are part of the Sensitivity and Uncertainty Analysis Element, and were the main focus of this study. The determination of the effect of the reactor input parameters and operating state on the output FOM occurs in *Step 11*, and non-parametric biases are determined (e.g., a typical thermocouple drift would not be included as a statistical variation, but as a constant off-set or bias). In *Step 12* parametric sensitivity calculations are performed to evaluate the impact of inputs on the FOM, and the determination of the combined bias and uncertainty variations is performed in *Step 13*. The actual determination of the total uncertainty is performed in *Step 14*, and can be done in several ways, e.g. simple random (or Latin Hypercube) Monte Carlo sampling of the selected parameters' distributions, response surface generation, etc. Two of these methods are discussed in some detail in the next section.

Two major approaches to perform uncertainty propagation in a statistically rigorous manner can be identified (Salah 2006):

1. Methods based on the propagation of *input* uncertainties (or statistical methods) as represented by the SUSA and DAKOTA (<http://dakota.sandia.gov/index.html>) codes
2. Methods based on the propagation of *output* uncertainties (or deterministic methods) of which the Capability of Internal Assessment of Uncertainty method (D'Auria, 2000).

The two approaches can be summarized as follows:

- Statistical methods (input uncertainty propagation) include:
 - Use of a reduced number of uncertain input parameters, i.e., non-significant parameters can be excluded.
 - Assign subjective probability ranges and distributions to these parameters.

- Propagate the combined uncertainty through the core models to determine the statistical properties of the FOM's Probability Density Function (PDF).
- Deterministic methods (output uncertainty propagation) include:
 - Use of a relevant set of experimental data to establish a database of uncertain data for a large number of input parameters.
 - Create hypercubes characterizing physical parameters for a wide variety of plant conditions, transients, etc.
 - Perform a single calculation utilizing all input parameters to determine the error bands enveloping the output FOM.

Both methods have advantages and drawbacks as shown in Table 1. Typically, because of the deterministic method requirement to have a large and comprehensive experimental database available, light and boiling water reactor uncertainty studies can use this method (especially for thermal fluid uncertainty studies). However, in the high temperature reactor domain, very limited experimental and operational data exists, and the use of statistical uncertainty methods is currently the only viable approach for coupled uncertainty propagation.

Table 1. Comparison between statistical and deterministic uncertainty assessment methodologies.

Method	Advantage	Disadvantage
Statistical	<ul style="list-style-type: none"> • Possible to use reduced number of code calculations (Wilks' formula) that is independent of number of uncertain inputs • Provides well-defined statistical data properties on output parameter's PDF 	<ul style="list-style-type: none"> • Subjective selection of uncertain input parameters • Subjective selection of uncertainty distribution types and ranges • Requires significant number of model calculations (typically ~59–153)
Deterministic	<ul style="list-style-type: none"> • Requires only a single calculation to provide continuous error bands for any output variable of interest 	<ul style="list-style-type: none"> • Requires a relevant experimental/operational data base to construct hypercubes • Major contributors to uncertainty error bands not distinguishable

2. FEATURES OF THE GRS STATISTICAL UNCERTAINTY METHOD AND SUSAS

The first step in the GRS method is to select the set of uncertain input parameters that will be used to evaluate the desired FOM. Information from the manufacture of nuclear power plant components as well as from experiments and previous calculations are used to define the mean value and probability distribution or standard deviation of uncertain parameters. Uniform (and in some cases normal) distributions are used in the absence of more knowledge about the input parameters. Once these distributions and dependencies have been established, the analyst can:

- Generate a random sample of size N ($N = 93$ for typical 5% lower and 95% upper percentile values), with a 95% confidence level (see Equations (1) and (2) below) for the input parameters from its probability distributions by a Monte Carlo module contained in the SUSAS package.
- Perform the corresponding N simulations with the codes. Each simulation generates one possible solution of the model. All solutions together represent a sample from the unknown probability distribution of the model results.
- Calculate quantitative uncertainty statements, e.g., 5 and 95% quantiles or two-sided statistical tolerance limits like upper and lower limit values with 95% coverage and 95% confidence (denoted here as [95%,95%]).
- Calculate quantitative sensitivity measures to identify those uncertain parameters that contribute most to the uncertainty of the results.

The number of code calculations is determined by the requirement to estimate a tolerance and confidence interval for the quantity of interest. Wilks' formulae (Wilks 1941) are used to determine the number of calculations required to obtain the desired uncertainty bands:

$$1 - a^n \geq b \tag{1}$$

$$(1 - a^n) - n(1 - a)a^{n-1} \geq b \tag{2}$$

Equations (1) and (2) are used for one-sided and two-sided statistical tolerance intervals, where $(b \times 100)$ is the confidence level (%) that the maximum code result will not be exceeded with the probability $(a \times 100 [\%])$ (percentile) of the corresponding output distribution, and n the number of calculations required. For example, for a 95% probability that the peak fuel temperature lies below the maximum value of the (unknown) peak fuel temperature distribution, and given with a confidence level of 95%, a total of $n = 59$ calculations need to be performed. Put another way, the one sided 95th percentile value of the (unknown) peak fuel temperature distribution is obtained with a confidence level of 95% by selecting $n=59$, and the same number of runs would be needed for the 5% percentile. If both percentiles are required, 93 runs would be required for the (95%,95%) two-sided tolerance limits.

It is important to note that the GRS method does not generate the distributions of output parameters. Rather, it yields two-sided limit values (coverage) with a user-specified confidence. For example, a SUSAS application may lead to the statement: "The analysis indicates with 95% confidence that in 95% of the cases the peak fuel temperature will be lower than 1600°C." It also ranks the input parameters according to the effect that its uncertainties have on the uncertainty in the output parameter, as part of the sensitivity analyses.

In summary, SUSAS is a program that performs a statistical analysis of uncertainty in the output of nuclear systems codes. Among its functions, SUSAS:

- Generates sets of input parameters given user-supplied distributions and input variable dependencies. The number of sets is a function of the confidence required in the uncertainty of the specified output parameters
- Can be programmed to write system code input decks for these parameters sets
- Can be programmed to execute the corresponding models using appropriate calls to the system code
- Performs a statistical analysis of the specified output parameters, correlates the uncertainty in the output to each of the input variables, and ranks the importance of each input variable to the output uncertainty.

The main advantage of the SUSAS software is that it allows a core analyst to apply the sophisticated statistical techniques required of the GRS method without actually having to code them, i.e., SUSAS can be used as a black-box wrapper. Because no code modifications are required, the method is entirely suitable for use with existing and older legacy codes. (A possible issue for regulatory acceptance could be the use of Microsoft Excel as the chosen SUSAS interface. However, since Excel is just used as a user interface - the statistical engine is coded in Visual Basic - verification and validation of SUSAS's methods can still easily be performed, if required).

3. SUS A TEST CASE: PEBBED-THERMIX DLOFC

The following target objectives were proposed for this study:

1. Obtain and install SUS A, and perform tutorial test cases and verify the installation
2. Define and execute an INL-specific test case using the PEBBED code to calculate the PBMR 400 Exercise 2 benchmark steady-state and DLOFC transient
3. Use SUS A to generate the statistical input data variations needed to produce a (95%,95%) statement for the peak fuel temperature as the FOM
4. Perform the required 93 PEBBED runs
5. Perform an uncertainty analysis with SUS A to obtain the (95%,95%) two-sided tolerance limits
6. Perform a sensitivity study with SUS A to obtain correlation data between the input and output parameters
7. Objectives 1 and 2 were discussed in the first revision of this report (INL-EXT-10-19023, June 2010), and a detailed discussion of the remaining five objectives are provided here.

Table 2 provides an overview of the test platform and software details utilized for this study.

Table 2. Test platform and SUS A code details.

Description	Platform/code details	Remarks
Hardware	DELL laptop, Intel duo CPU @ 2.66 GHz, 3.5 GB RAM	
Operating system	Windows XP Professional, version 2002, Service pack 3	
SUS A software	Version 3.6	There is no indication in the code release documentation that the SUS A “evaluation” or “trial” version released to INL actually differs from the “commercial” version 3.6. All the available functionalities described in the commercial code’s user manual are active for testing.
Additional required software (1)	SUS A uses a macro graphical user interface (GUI) through MS Excel, and both 2007 and 2003 versions are supported. Excel 2007 versions do however need additional .dll patches from the Microsoft website.	For this report, MS Excel 2003 Professional build (11.8320.38221) SP3 was used.
Additional required software (2)	SUS A provides a FORTRAN 90 “wrapper” or shell as part of the software package. This shell enables internal calls to the user code, which can then be compiled as a single executable. A FORTRAN compiler is then required. No FOTRAN prescriptions are provided from SUS A’s side, but it is known that GRS uses COMPAQ Visual FORTRAN version 6.6 for their development testing.	The internal coupling approach (i.e., calling PEBBED internally with SUS A controlling the serial runs) was not tested at INL. The external model runs method was used for this study (see Figure 2).

Figure 2 presents a simplified flow diagram of the methodology followed for the PBMR 400 Exercise 2 benchmark test case.

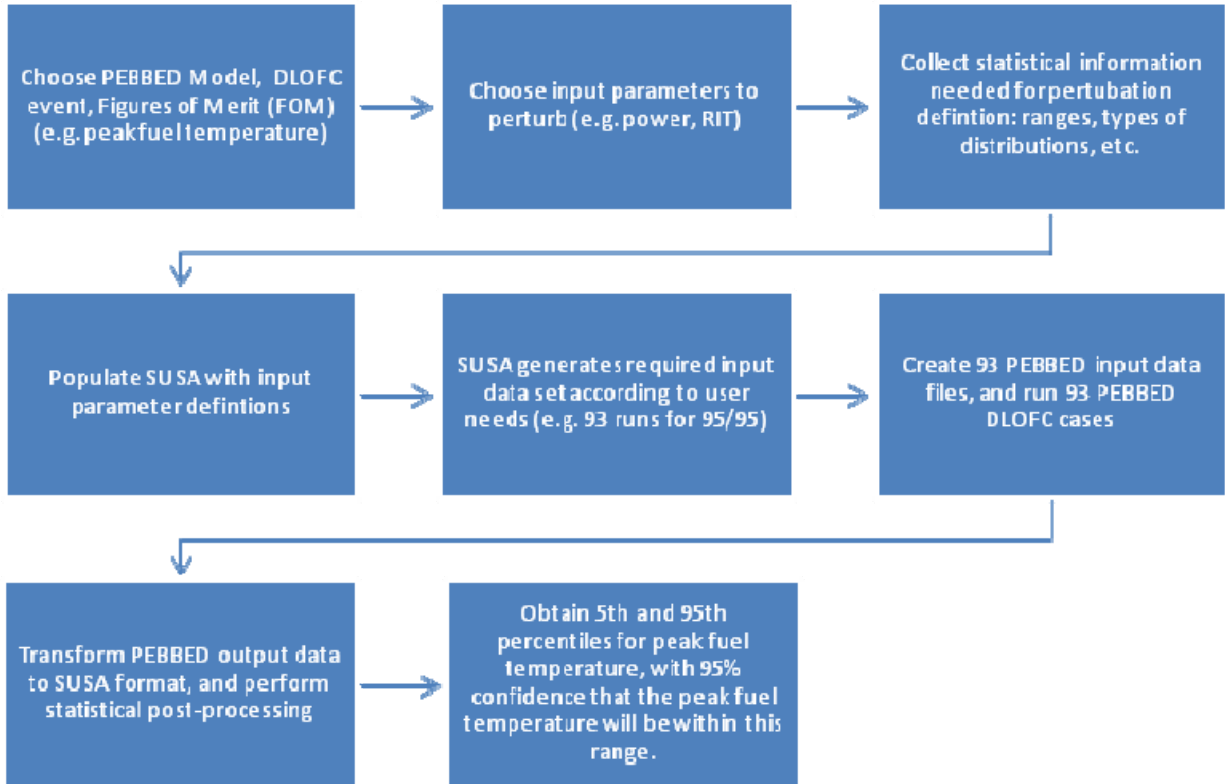


Figure 2. Example of the GRS methodology applied to the PEBBED CRP-5 PBMR 400 Exercise 2 benchmark calculation.

The results of PEBBED-THERMIX uncertainty and sensitivity analysis are presented in the following six subsections based on the sequence shown in Figure 2.

3.1 Code, Model, and FOM Selection

As already indicated earlier, the capabilities of the PEBBED-THERMIX code suite was investigated to determine if the codes can be used for a typical DLOFC transient. After this was confirmed, an existing model of the CRP-5 PBMR400 (Gougar 2010b) was used as the starting point of the uncertainty study.

The typical FOM for a DLOFC event is the peak fuel temperature, i.e., the maximum spatial and temporal temperature reached in the fuel spheres. This will usually be the time dependent behavior of a single region in the core (except for the first 24 hours of the transient, when this location is not fixed and still moving upwards in the core). The normal operation (or steady state) maximum fuel temperature and the daily fuel loading rate were also tracked as secondary FOMs, since these two parameters were also influenced to a lesser degree by the variances in the input data.

3.2 Input Parameters, Distribution Types and Variations

As an illustration of SUSA’s capabilities, eight input parameters were selected for this study, as shown in Table 3. Since the selection of the input parameters to be perturbed is one of the potential weak points of the statistical uncertainty methodology, the results of a separate TINTE study (performed for the PBMR design [Strydom 2004]) was used to determine which eight parameters to include for this PEBBED DLOFC case.

Table 3. PEBBED CRP-5 DLOFC uncertainty study input parameters.

Parameter	Mean value	2 Standard deviations (2σ) value	PDF Type
Reactor power	400 MW	±8 MW (2%)	Normal & Uniform
Reactor inlet gas temperature (RIT)	500°C	±10°C (2%)	Normal & Uniform
Decay heat multiplication factor	1.0	±0.057 (5.7%)	Normal & Uniform
Fuel specific heat multiplication factor	1.0	±0.06 (6%)	Normal & Uniform
Reflector specific heat multiplication factor	1.0	±0.10 (10%)	Normal & Uniform
Fuel conductivity multiplication factor	1.0	±0.14 (14%)	Normal & Uniform
Pebble bed effective conductivity multiplication factor	1.0	±0.08 (8%)	Normal & Uniform
Reflector conductivity multiplication factor	1.0	±0.10 (10%)	Normal & Uniform

This study indicated that metal and graphite emissivity only influenced the metal component temperatures, and uncertainties in the helium thermal physical properties also did not result in any changes in the FOM. Out of 19 input parameters investigated in the TINTE study, six had no effect on the steady-state and DLOFC maximum fuel temperatures, eight had less than 10°C (0.6%) effect, and only five factors resulted in changes larger than 10°C in the DLOFC FOM. These five input variables, together with three more that had a larger than 1% influence on the steady-state temperature, were selected for inclusion in this study.

The variations on the power and reactor inlet gas temperature were applied directly on the absolute value of the input variable itself (e.g., 2% on 400 MW), in contrast to the decay heat, specific heat, and thermal capacity variations where the variations were applied as multiplication factors on the complex correlations that are used to calculate these variables. For example, the specific heat capacity of the reflector graphite material is a third-order polynomial function of temperature T and the density ρ where

$$c_p = \rho (0.645 + 3.14 T + 2.809 T^2 + 0.959 T^3) \quad (3)$$

The sampled multiplicative factor c_{p_mod} is then applied to the interim value to determine the final specific heat value in

$$c_p = c_{p_mod} * [\rho (0.645 + 3.14 T + 2.809 T^2 + 0.959 T^3)] \quad (4)$$

The mean and two standard deviations (2σ) values shown in Table 3 were obtained from material manufacturers (specific heat and conductivity data), expert engineering judgment (power and inlet temperature), and from established industry standards (decay heat).

The GRS methodology and, specifically, the use of Wilks' method does not require the use of a limited number of perturbed input parameters; if required, all possible input variations can be taken into account without an additional calculational burden. (In the BEMUSE benchmark, the various participants selected between 11 and 64 input parameters to vary, and all but one participant performed only 93 model calculations). A large number of input parameters do, however, imply a significant effort to quantify the distribution type and variances for each of these parameters. Since the intention of this study is only to demonstrate the capabilities of SUSA, as opposed to a safety case study by a reactor vendor, it was

decided that the eight most influential parameters, as determined by the TINTE study, will be included here.

A second potential weak point of the statistical method is the justification for the selection of the PDF types. Typical thermal physical properties, such as specific heat and thermal conductivity, can be obtained from the manufacturers, and are usually specified as normal PDFs with mean standard deviation values. More complex variable PDFs (e.g., variations in the core bypass flows) can be biased/skewed to one side, as when gap widths grow larger or shrink over time or a preferred direction of thermocouple measurement drifts as it ages. In cases where no definitive uncertainty information exists, a simple uniform PDF can be assigned (all values within a certain range are equally probable, as indicted by Glaeser [2008]), or a standard/Gaussian PDF can be used with or without truncated tails. For this study, both normal and uniform PDFs were selected to assess if this factor plays a significant role in the DLOFC maximum fuel temperature uncertainty (see Table 4).

3.3 SUSAs Statistical Input Data Generation

The information required by the SUSAs code is entered via a Microsoft Excel Graphical User Interface (GUI). The process starts at the definition of the variable names and PDF information, as shown in the SUSAs GUI dialogue at this point (Figure 3).

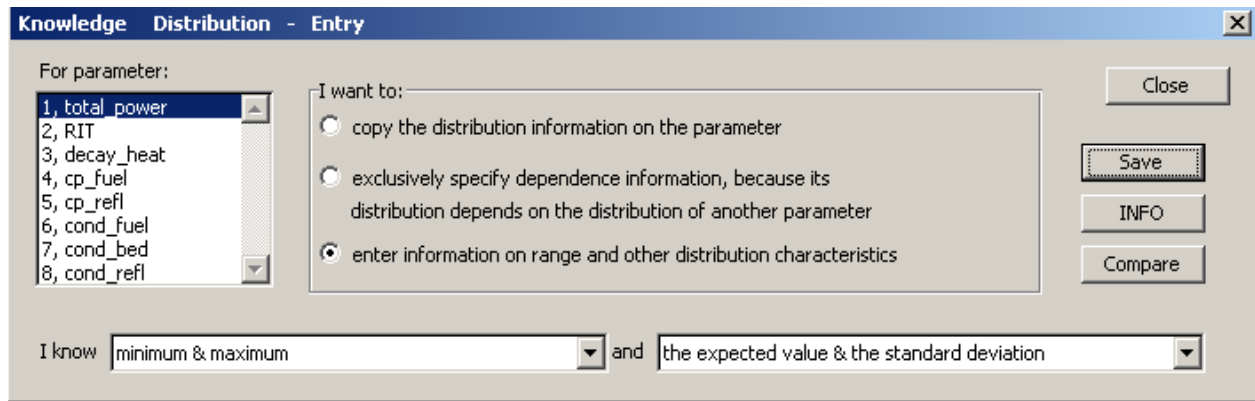


Figure 3. SUSAs input parameters distribution information entry screen.

The next step provided detailed information for each of the input parameters. Figure 4 presents the data for the Total Power input variation, with a normal distribution selected and the mean and standard deviation values specified. Note that infinite tails of the normal distributions were all truncated at their 2σ values (at the 95.5% percentiles) to enable direct comparison with the uniform distributions' minima and maxima. A visual check on the calculated PDFs and cumulative distribution functions are provided by selecting the "plot" option, as shown in Figure 5 to Figure 7.

Knowledge Distribution - Quantification

Parameter 1, total_power

Distribution Type: Density f(x) = $1/(p2*\sqrt{2*PI}) * \exp(-0.5*((x - p1)/p2)^2)$

Par. p1: Par. p2 (>0):

Minimum: Maximum:

Expected Value: Std. Deviation:

Figure 4. SUSA entry screen for “Total Power” distribution information.

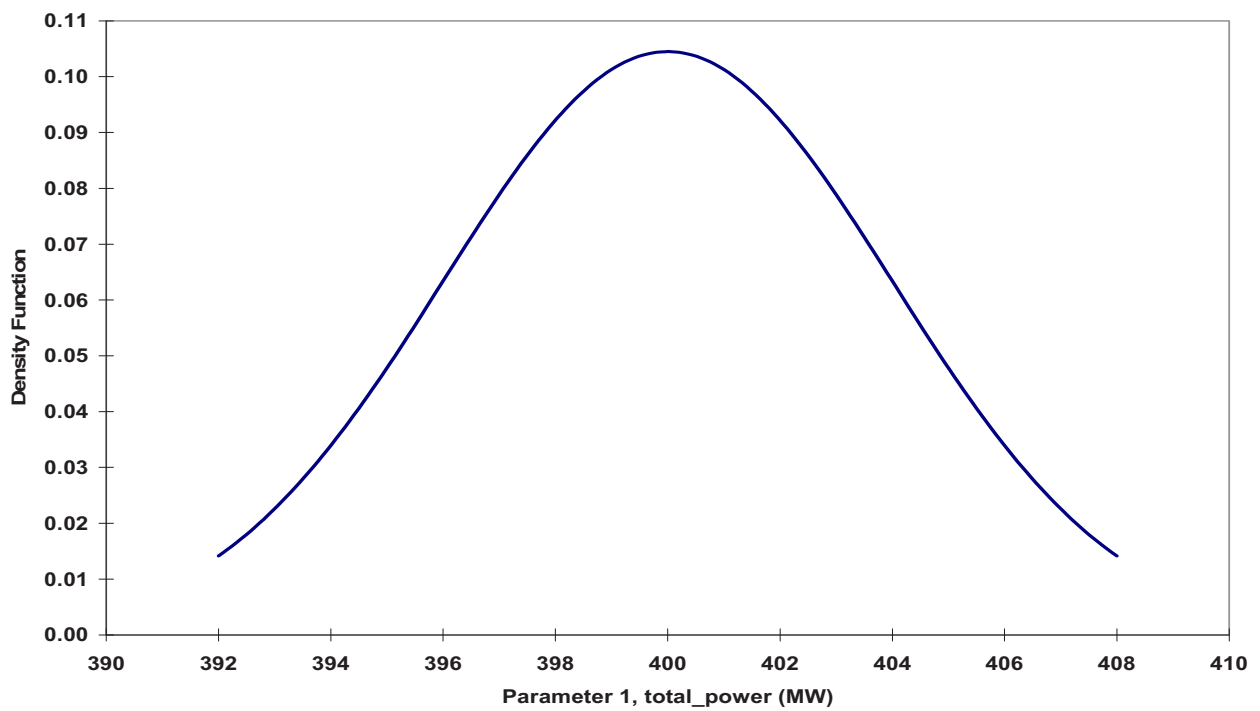


Figure 5. PDF for the total power input parameter.

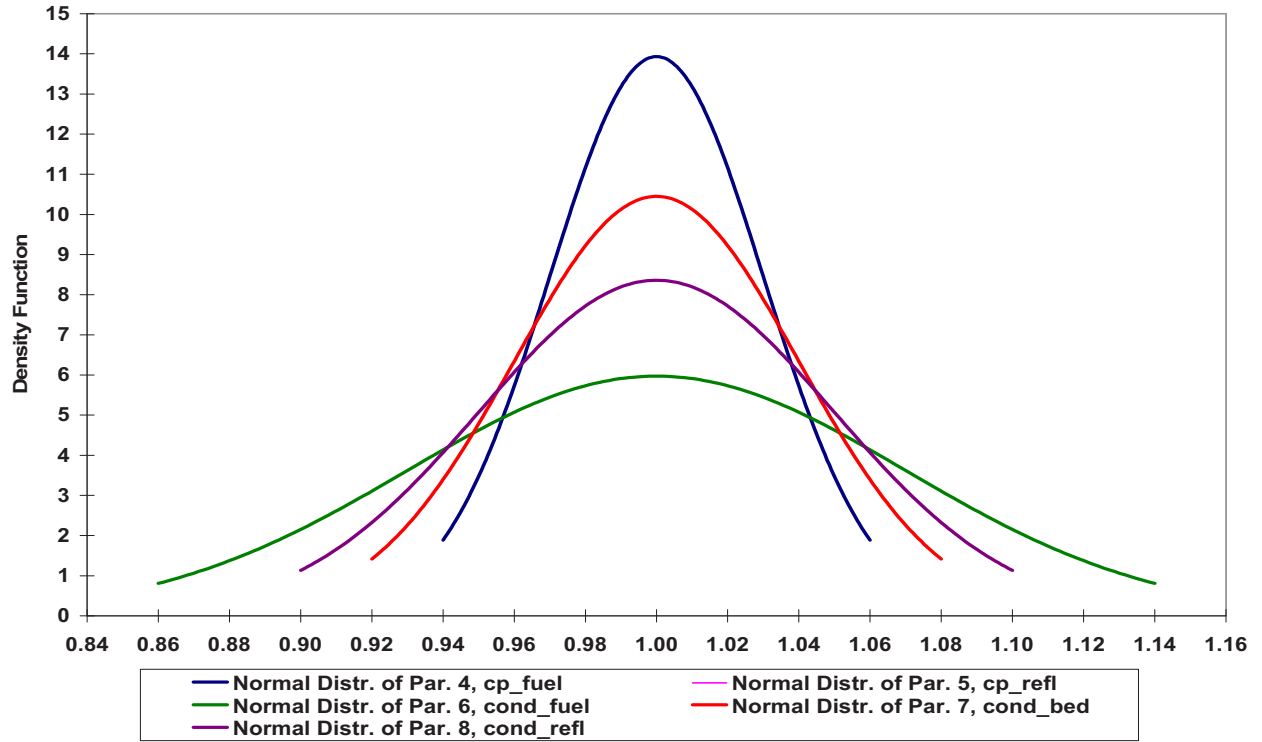


Figure 6. PDFs for the specific heat and thermal conductivity correlation input parameters.

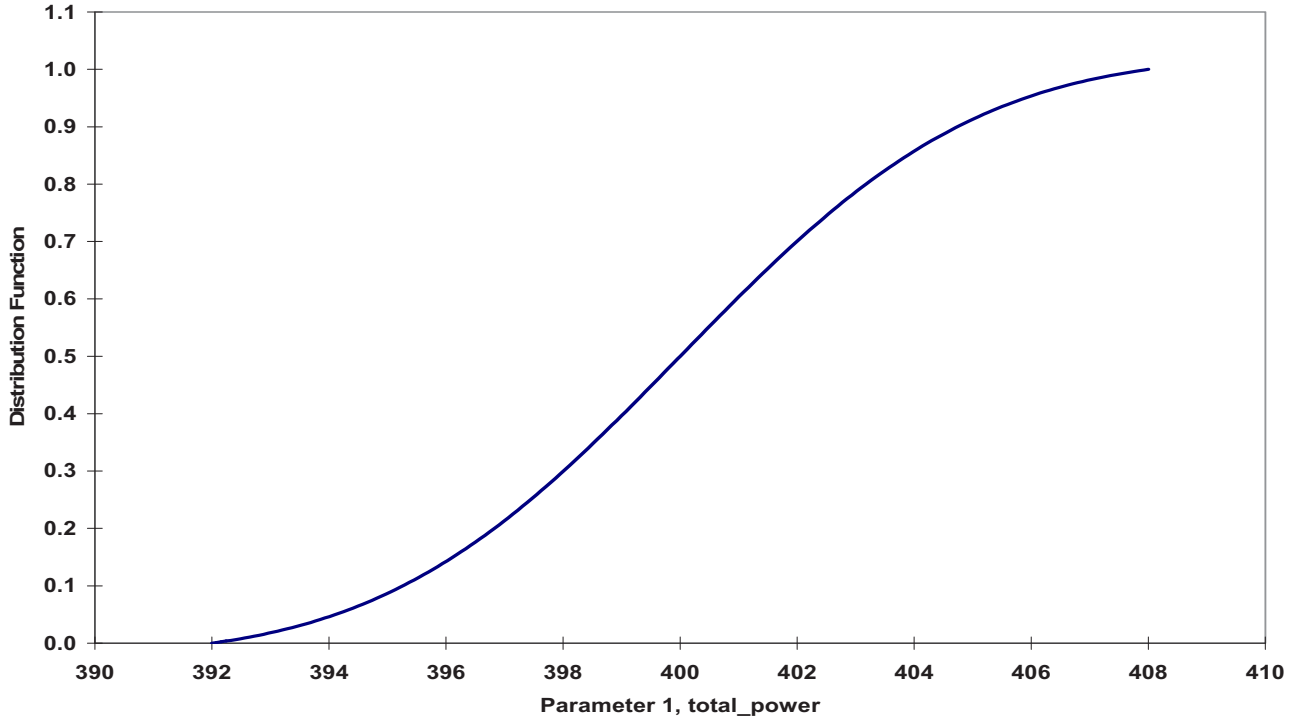


Figure 7. Cumulative density function for the total power.

A total of six SUSA case sets were performed for this study as described below and summarized in Table 4:

- The number of model runs were varied between 100 and 200 to investigate if double the required model runs (93) produced a smaller or larger DLOFC maximum fuel temperature uncertainty estimate.
- SUSA is capable of using either the simple random sampling (SRS) (Yates 2008) or the Latin hypercube sampling (LHS) method (McKay 1979) for generating the values of the input variables from their specified distributions. A final set of 200 model runs was performed to compare the FOM uncertainty estimates generated by these two sampling methods.
- As indicated in Section 4.2, both the 100 and 200 model run sets were repeated with uniform and normal distribution types.
- A final point of interest was the uncertainty contribution of a few dominant input parameters compared to the combination of all eight input parameters. To this end, two sets of 100 model runs each were performed, varying only the material correlations and only the power, RIT, and decay heat correlation, respectively.

Table 4. PEBBED-THERMIX CRP-5 DLOFC uncertainty study cases.

Number of Model Runs	Input Parameter Sampling Method	Input Parameter Distribution Type	Model Input Parameters Varied
100	Latin Hypercube	Uniform	Power, RIT, decay heat only
100	Latin Hypercube	Uniform	Specific heat and thermal conductivity only
100	Latin Hypercube	Uniform	All
100	Latin Hypercube	Gaussian/Normal	All
200	Latin Hypercube	Gaussian/Normal	All
200	Simple Random	Gaussian/Normal	All

In the discussions that follow, the notation will be of the format “number, sampling method, distribution type”; for example, the first and last entries in Table 4 will be referred to as *100 LHS Uniform* and *200 SRS Normal*.

In the SUSA application, both the SRS and LHS methods use a random six-digit number as “seed” for the generation of random numbers between 0.0 and 1.0, which are then used to sample parameter values from their respective PDFs as shown in Figure 8. The user can also request several statistical indicators on the correlations between the input parameters, for example the Pearson (Rogers 1988) and Spearman (Maritz 1981) coefficients, to confirm that unintended dependencies between the random input sample sets did not occur.

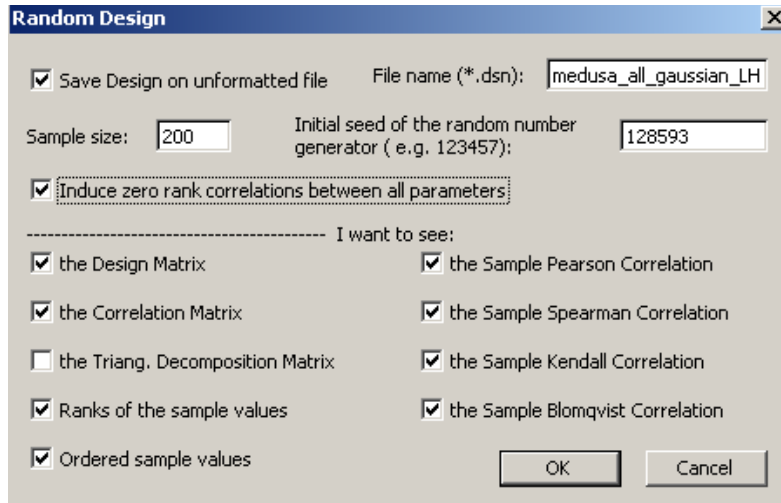


Figure 8. SUSA random generator GUI dialogue.

An example of the final outcome of this input preparation phase is shown in Table 5, where the values of the eight input parameters are presented for the first 10 of the 200 LHS Normal set model runs.

Table 5. PEBBED-THERMIX input data for the first 10 model runs of the 200 LHS Normal set.

Reactor Power (MW)	Inlet gas Temperature (°C)	Decay heat multiplier	Fuel specific heat multiplier	Reflector specific heat multiplier	Fuel conductivity multiplier	Bed conductivity multiplier	Reflector conductivity multiplier
393.9	497.5	0.995	0.977	1.023	0.976	1.029	1.064
400.2	501.1	0.977	1.006	0.998	1.004	0.987	1.012
397.6	507.0	1.040	0.947	0.948	0.945	1.011	1.055
393.6	498.4	1.048	0.974	1.029	0.955	1.016	1.035
401.9	496.8	1.002	0.951	1.004	0.947	1.024	1.080
403.6	499.6	0.969	1.018	0.996	1.092	1.054	1.039
398.2	505.0	0.973	0.980	0.962	0.912	0.999	0.964
399.3	499.8	0.958	0.987	0.928	1.095	0.975	1.028
405.6	503.8	0.981	0.979	0.984	0.958	0.964	0.903
400.4	500.6	0.984	0.966	0.954	1.020	1.025	1.085
398.5	494.1	0.956	1.013	0.946	1.013	0.995	0.947

The SUSA generated input data can also be verified for conformance to the user's specifications using scatter plots. Two sample scatter plots are shown in Figure 9 (total power) and Figure 10 (reflector conductivity multiplication factor) for the 200 LHS Normal set.

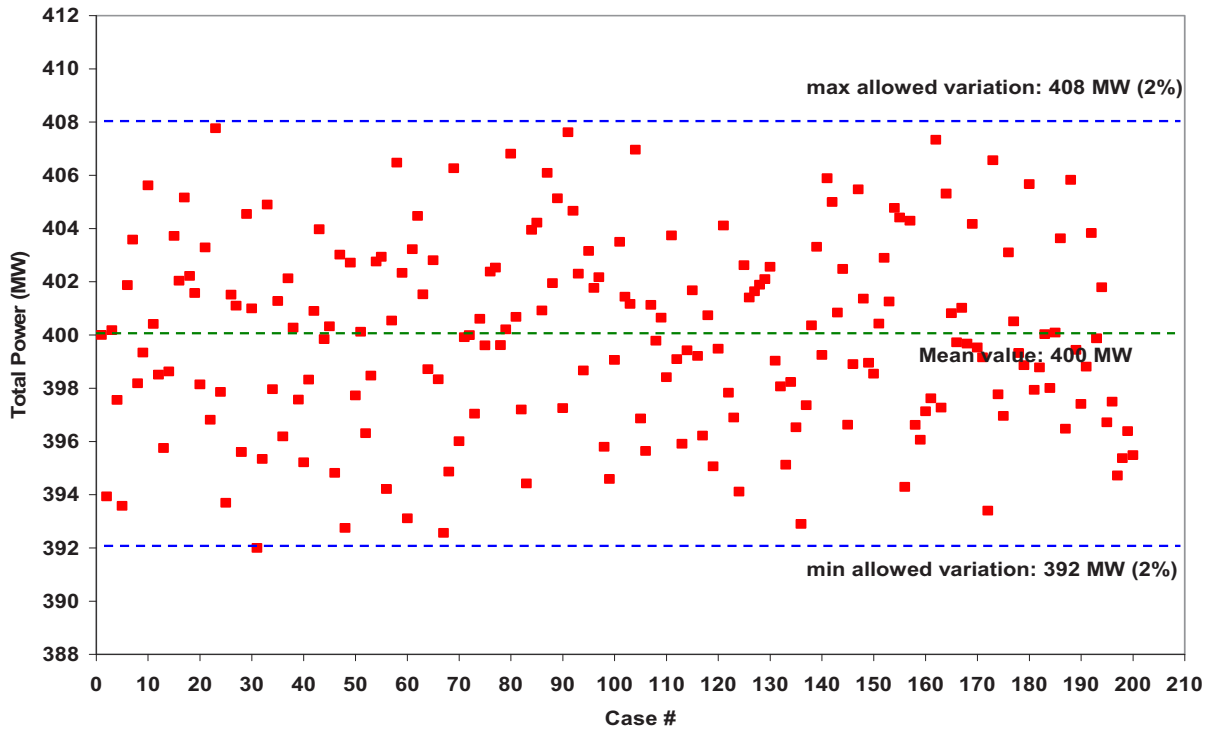


Figure 9. Sampled values of the total power (MW) for the 200 LHS Normal set.

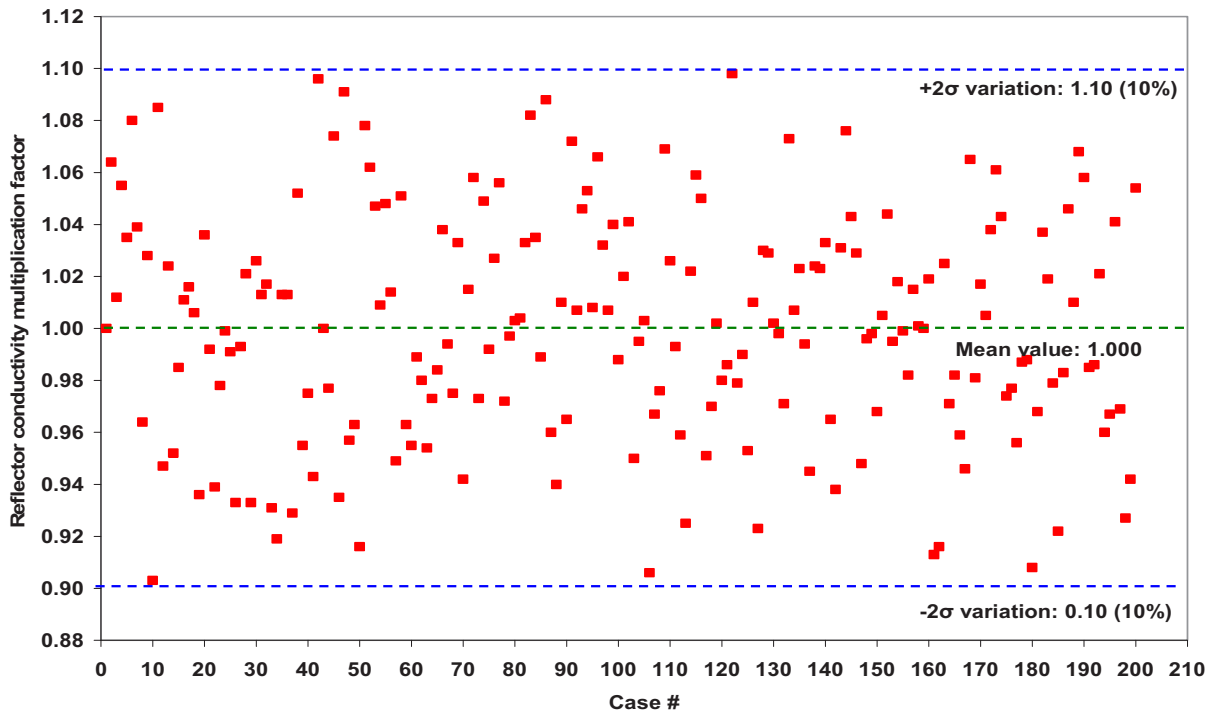


Figure 10. Sampled values of the reflector conductivity multiplication factor for the 200 LHS Normal set.

3.4 PEBBED-THERMIX Calculation Results

During the next step of the procedure, the SUSANA-generated data for the eight input parameters were used to create model input files for the PEBBED-THERMIX steady-state and DLOFC calculations. The six sets (Table 4) required 800 PEBBED calculations at an average run time of 35 minutes each on a single processor. While it is possible to assign the model runs to a multiprocessor system for a significant decrease in calculation times, the calculations were performed sequentially on a single machine. Because of the large volume of data generated by the 800 model calculations, only summarized comparative results are presented for most of the sets.

The time behavior of the maximum fuel temperature during the DLOFC transient is shown in Figure 11 to Figure 13 for the first 30 cases of the 100 SRS Uniform, 100 LHS Normal, and 200 LHS Normal data sets, respectively. (Note that the maximum fuel temperature is a *spatial* function, since the PEBBED-THERMIX model calculates temperatures in 110 core zones/meshes. The temporal maximum of this maximum fuel temperature during the DLOFC is defined as the *peak* fuel temperature. This spatial location moves upwards in the core by more than 5 meters in the first 15 hours, and as such the curves shown here do not represent the same location at all times - simply the highest fuel temperature at any given moment in any location.)

A few observations on the general trends can be made from this data:

- The PBMR core design leads to the typical high temperature reactor slow increase in the maximum fuel temperature over several hours, with the peak fuel temperatures reaching between 40 to 60 hours into the transient.
- The shapes of the curves in the first 30 cases are similar but the gradients are not. Although the same physical phenomena are present in all the DLOFC events, the rate of energy deposition (correlated to the decay heat) and energy removal (correlated to the fuel and reflector specific heat and thermal conductivities) differ for each of these cases, according to the sampled input values.
- Changes in the eight input parameters have opposite effects on the maximum fuel temperature; an increase in the decay heat will increase the fuel temperature, but an increase in the fuel graphite conductivity will remove heat faster from the core, and therefore lead to a lower fuel temperature (see also the Sensitivity Study, Section 4.6). Since each DLOFC case consists of a random sampled set of the eight input parameters, the low fuel temperature curves can be the result of a few parameters sampled low (or high) simultaneously, and an average fuel temperature curve could be caused by a cancellation of effects. This effect is also the cause of the shift in time when the peak fuel temperature values are reached.
- The spread in maximum fuel temperatures between the first 30 cases is not constant with time. For example, it starts off with less than 5°C in the first hour and increases to 98°C for the 200 LHS Normal set, as shown in Figure 13. This divergence over time is a direct result of the sampled input parameter values, as explained above. For a time dependent event such as this DLOFC, a single and constant fuel temperature uncertainty result can therefore not be expected - it will be a function of time as well. It can be seen in Figure 11 to Figure 13 that the temperature spread between the cases continue to increase after the peak values have been reached, and a full uncertainty study should take this effect into account if it is required to determine what the maximum uncertainty bandwidth is.
- Examples of the (95%,95%) two-sided tolerance limits are not provided at a fixed time point, but rather at the varying time point where a specific case reaches its peak DLOFC fuel temperature. The arrows in Figure 14 show that this time point occurs between 45 and 54 hours. This study therefore compares the bounding value fuel temperature uncertainty for the DLOFC event, regardless of when this point is reached, since the DLOFC peak fuel temperature is of major interest in reactor design safety studies.

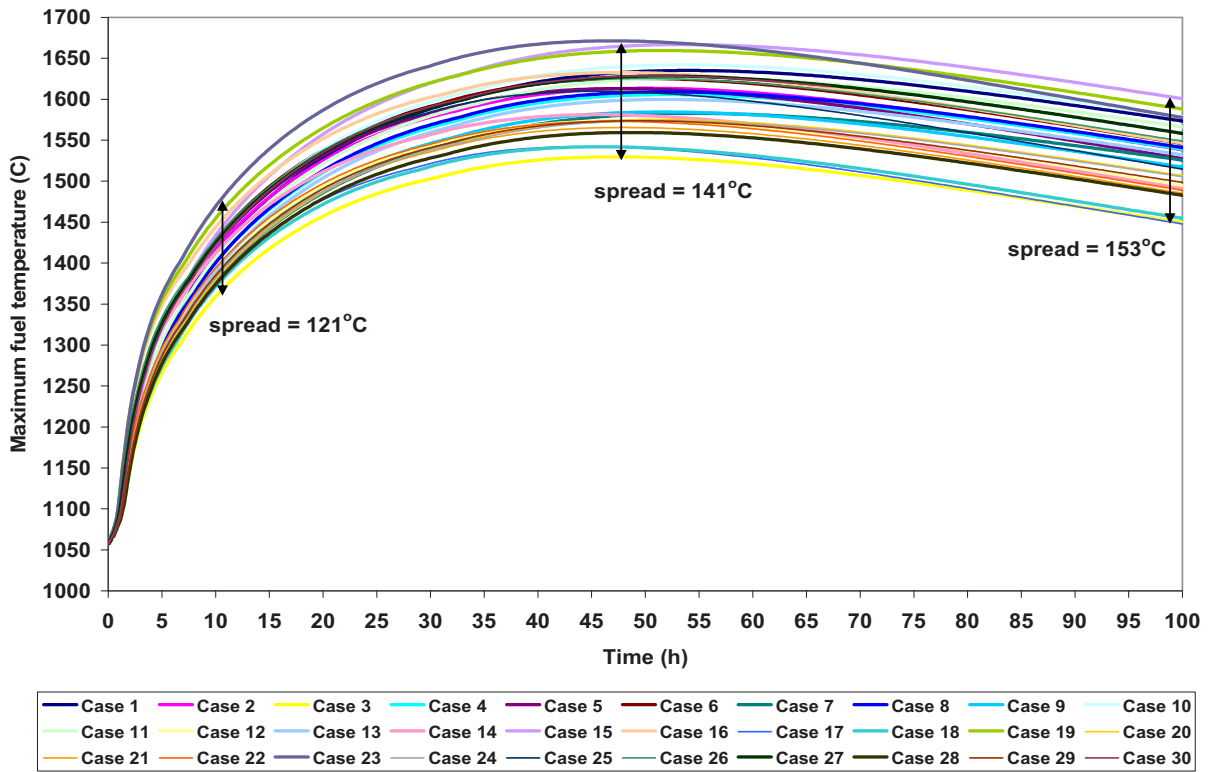


Figure 11. DLOFC maximum fuel temperature vs. time for the first 30 cases of the 100 SRS Uniform set.

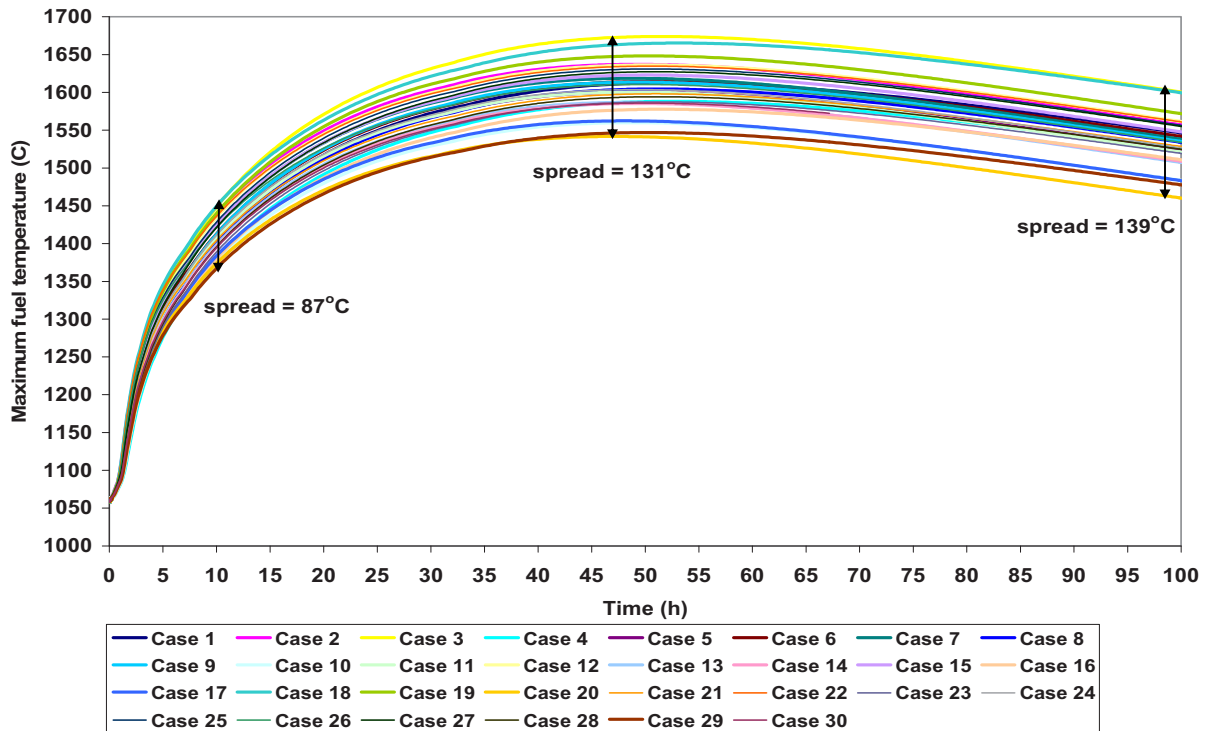


Figure 12. DLOFC maximum fuel temperature vs. time for the first 30 cases of the 100 LHS Normal set.

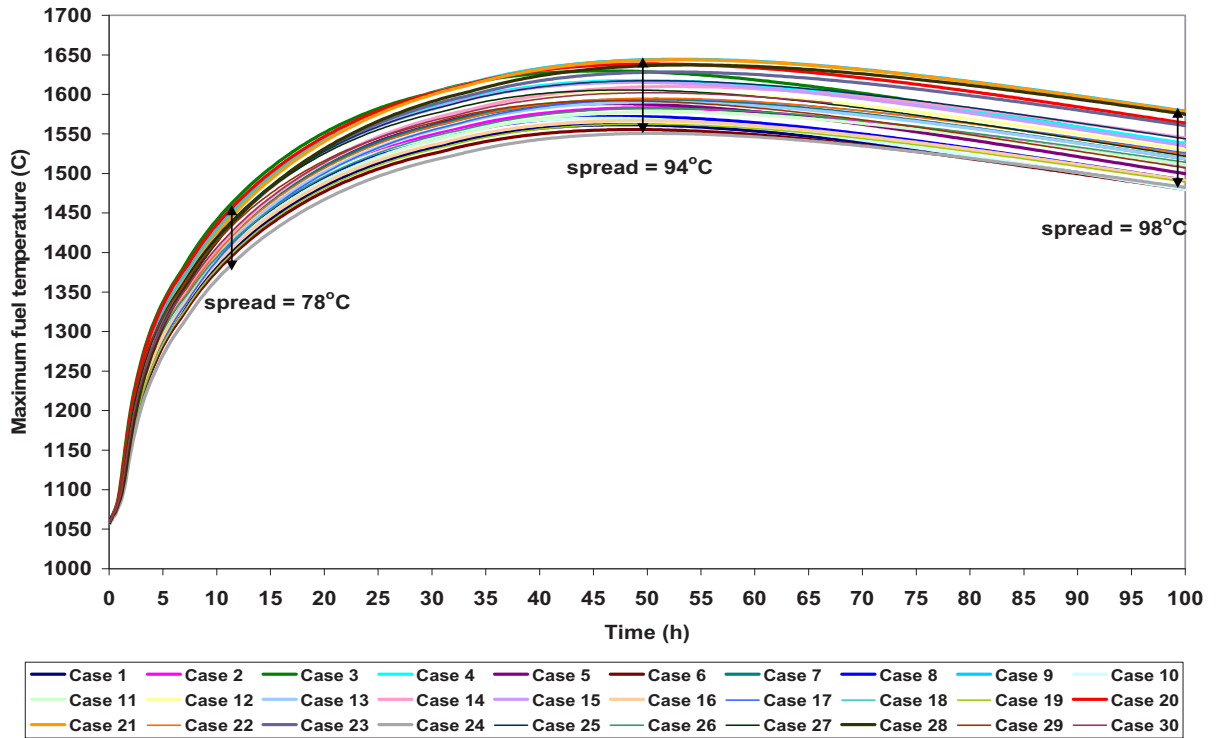


Figure 13. DLOFC maximum fuel temperature vs. time for the first 30 cases of the 200 LHS Normal set.

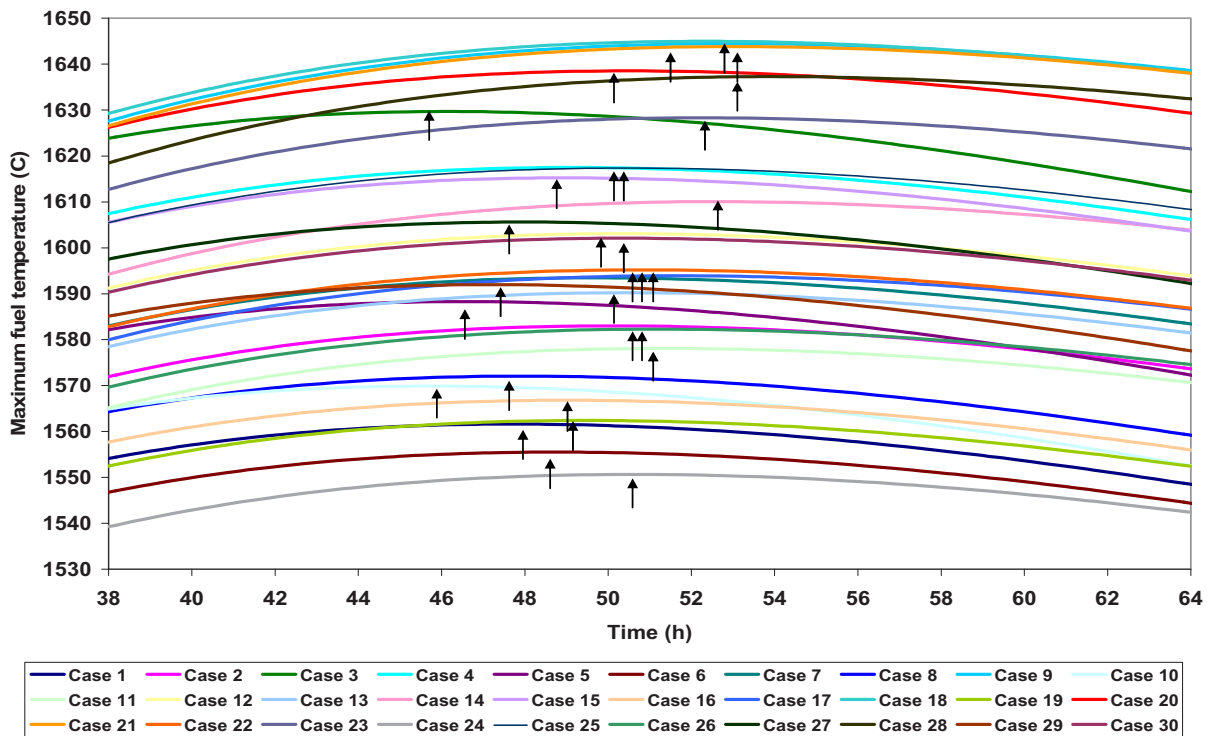


Figure 14. DLOFC maximum fuel temperature vs. time for the first 30 cases of the 200 LHS Normal set: detail of the peak temperature turning points.

- The temperature variation bandwidth for the 3 cases shown here is quite different. The two sets that consisted of 100 runs each produced significantly larger variations than the 200 LHS Normal set (e.g. 141°C vs. 94°C), and there is also a smaller difference between the 100 LHS Normal and 100 SRS Uniform sets (131°C vs. 141°C). This is caused by the random statistical sampling of the sets, and it is important to note that the figures just show the first 30 model runs of each set for clarity sake. For the 200 LHS Normal set, the remaining 170 model runs populates the final distribution further as shown in Figure 15, while Section 4.5 (Table 8) shows that the uncertainty estimates for the 6 full sets are very similar. This principle is illustrated by comparing Figure 12 and Figure 16, where a subset of 8 cases from the same SUSA set (100 LHS Normal) produces a much smaller variation compared to a subset of 30 cases.
- The primary FOM (DLOFC peak fuel temperature) and the two secondary FOMs (steady state maximum fuel temperature and the daily fuel loading rate) results are presented in Figure 17 to Figure 19 for the 200 LHS Normal set. The mean and $\pm 2\sigma$ values are also indicated in two of the figures. Table 8 shows that the (95%,95%) two-sided tolerance limits are almost identical to the $\pm 2\sigma$ values, since $2\sigma = 95.5\%$. The peak DLOFC fuel temperature and pebble load rate data for the 200 runs show a random behavior (no discernable pattern is seen between the various runs), but the steady-state fuel temperature seems to be clustered together in discrete bands. This is caused by integer rounding and the small scale of the variations: the (95%,95%) two-sided tolerance limits for the 200 runs differ only by 7°C around a mean value of 1082°C. Since PEBBED adjusts the fuel loading rate for each of these steady-state calculations to a targeted k-eff value of 1.0000, the steady-state temperatures will not vary significantly. The only output variables amenable to a statistical analysis are therefore the peak DLOFC fuel temperature and pebble load rates.

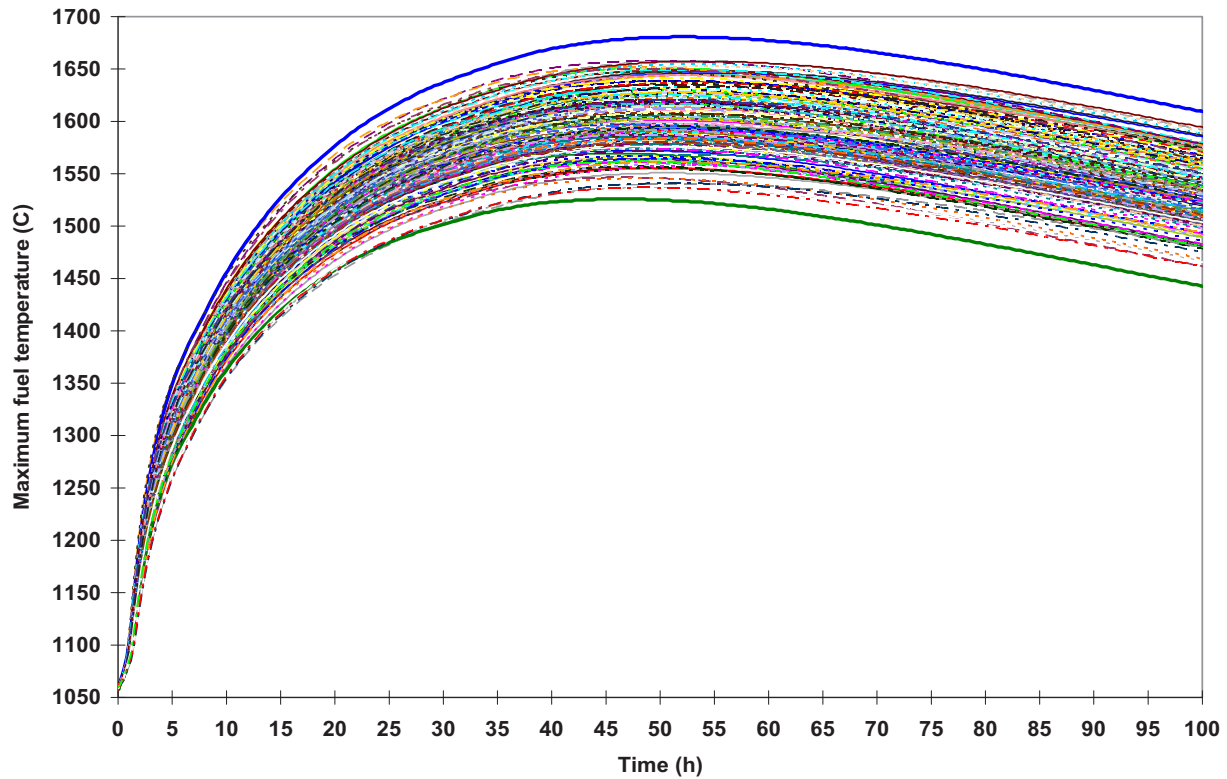


Figure 15. DLOFC maximum fuel temperature vs. time for all 200 cases of the 200 LHS Normal set.

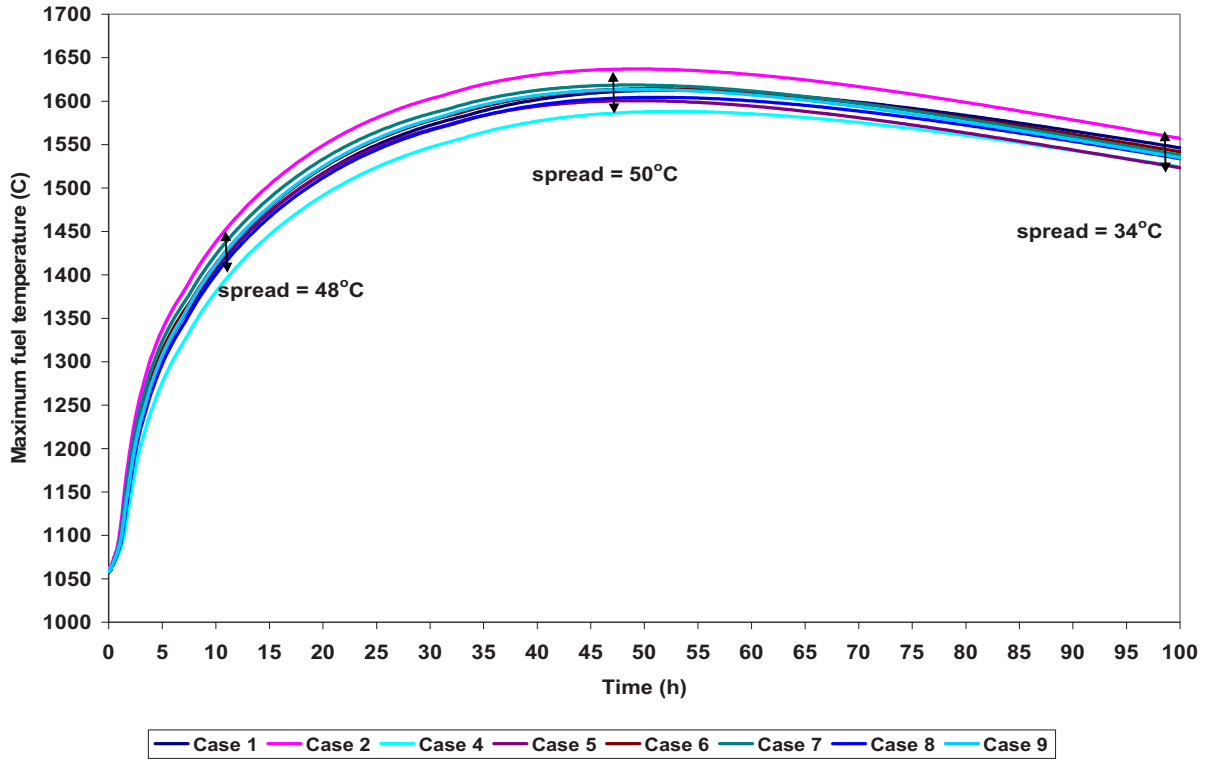


Figure 16. DLOFC maximum fuel temperature vs. time for eight cases of the 100 LHS Normal set.

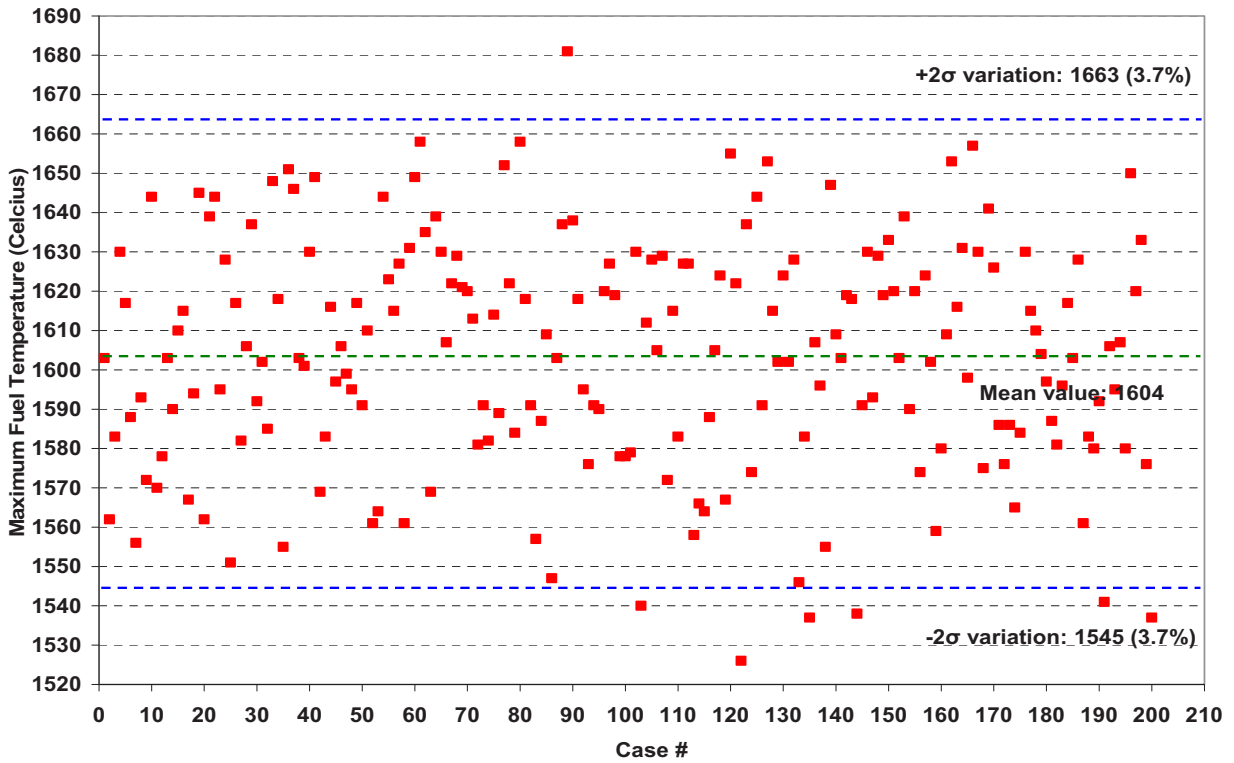


Figure 17. Maximum DLOFC fuel temperature of the 200 LHS Normal set at 50 hours.

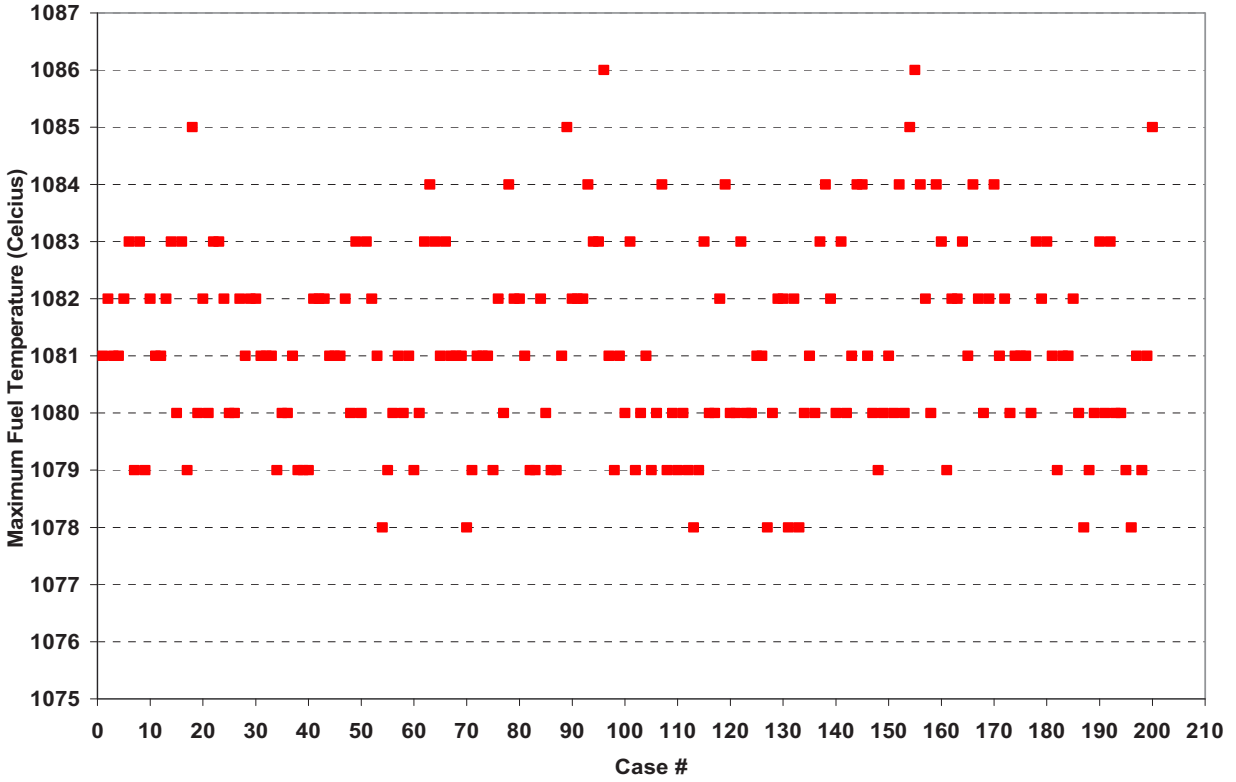


Figure 18. Maximum steady-state fuel temperature of the 200 LHS Normal set at 0 hours.

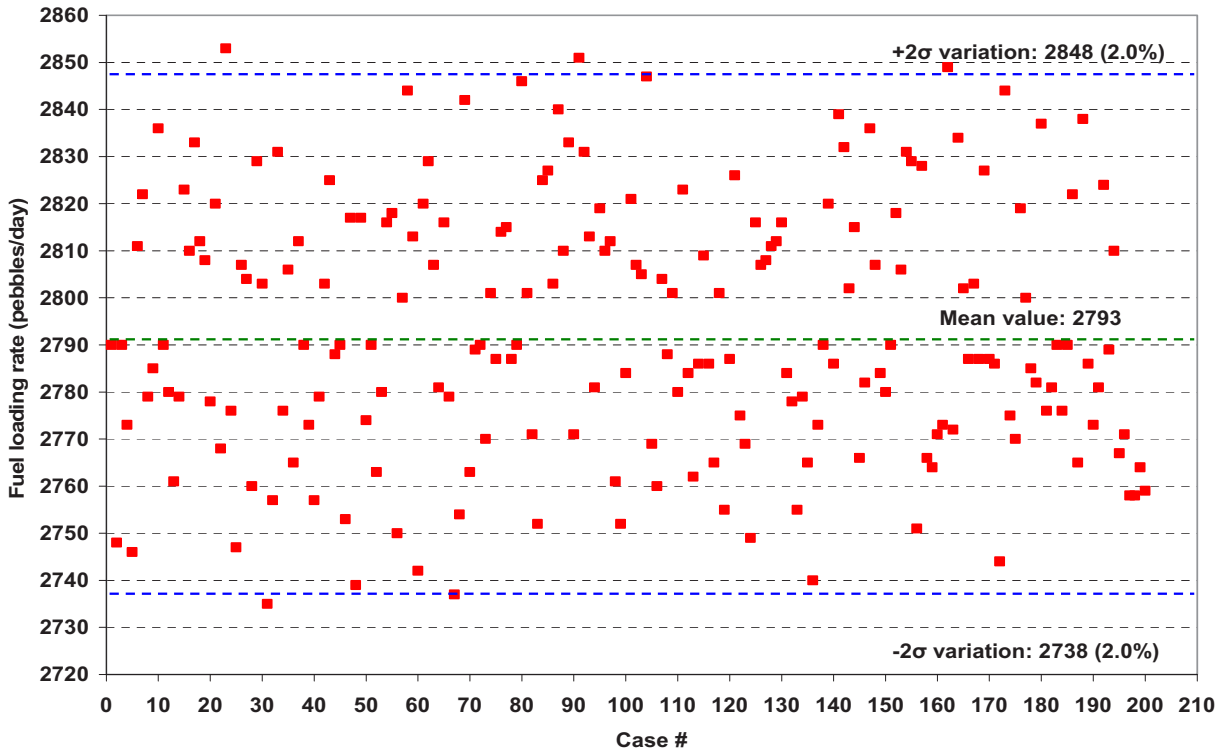


Figure 19. Daily fuel loading rate of the 200 LHS Normal set.

3.5 SUSA Uncertainty Analysis

For the uncertainty quantification step, SUSA can perform several statistical correlation fitness tests on the output data to determine the properties of the unknown statistical distributions. For example, the Kolmogorov-Smirnov (K-S) test (Chakravarti et al. 1967) quantifies the distance between the empirical distribution function of the sample and the cumulative distribution function of a reference distribution, and can be used to compare a population sample with a specific distribution (normal, log-normal, Weibull, uniform, Beta or Gamma). SUSA can also perform the Lilliefors test (Lilliefors 1967), which is a modification of the K-S test that tests for the normal, exponential or log-normal distribution types. Once a statistically significant distribution match has been found, the mean, standard deviation, and other indicators of the population can be determined.

An illustration of the K-S test application is shown in Figure 20 to Figure 22, where the peak DLOFC fuel temperature results of the 100 LHS Normal set is compared with SUSA fits of three possible distributions: Normal (Figure 20), Weibull (Figure 21), and Uniform (Figure 22). The quality of the fit can be visually assessed and the K-S values (0.9919, 0.2231, and 0.0026) confirm that a normal distribution is the closest match to the peak DLOFC fuel temperature data set.

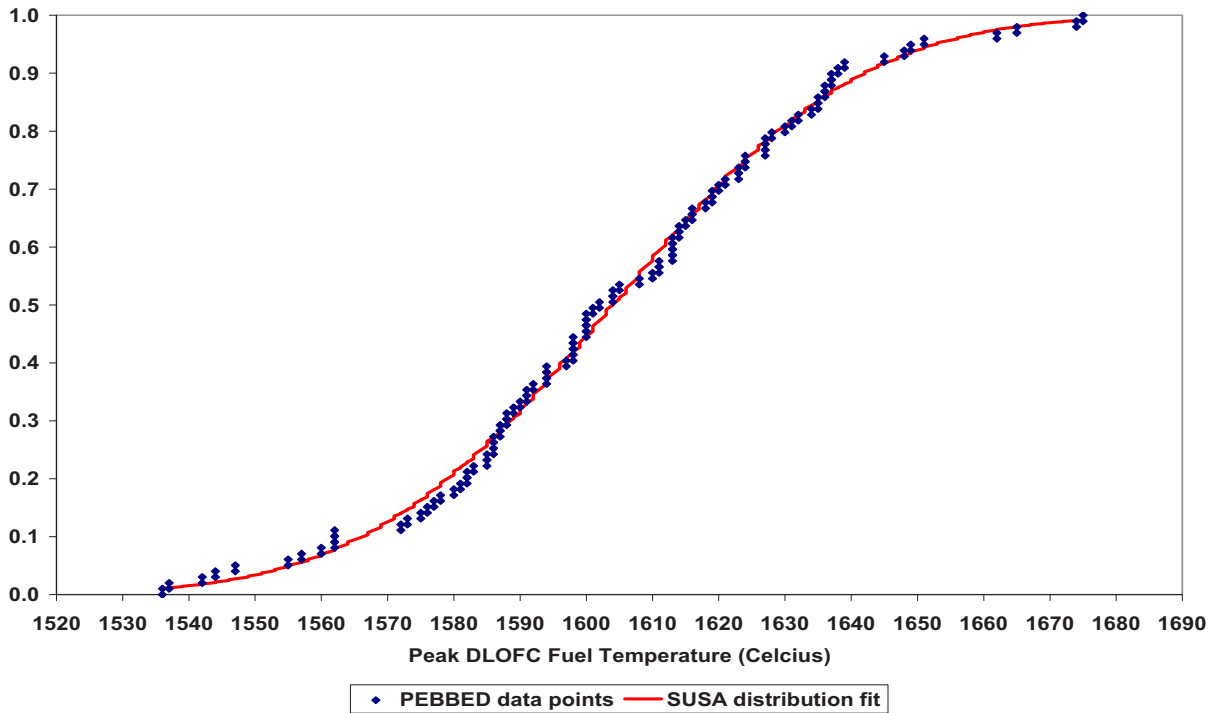


Figure 20. PDF and fitted normal distribution results for the 100 LHS Normal set: K-S level of significance = 0.9919.

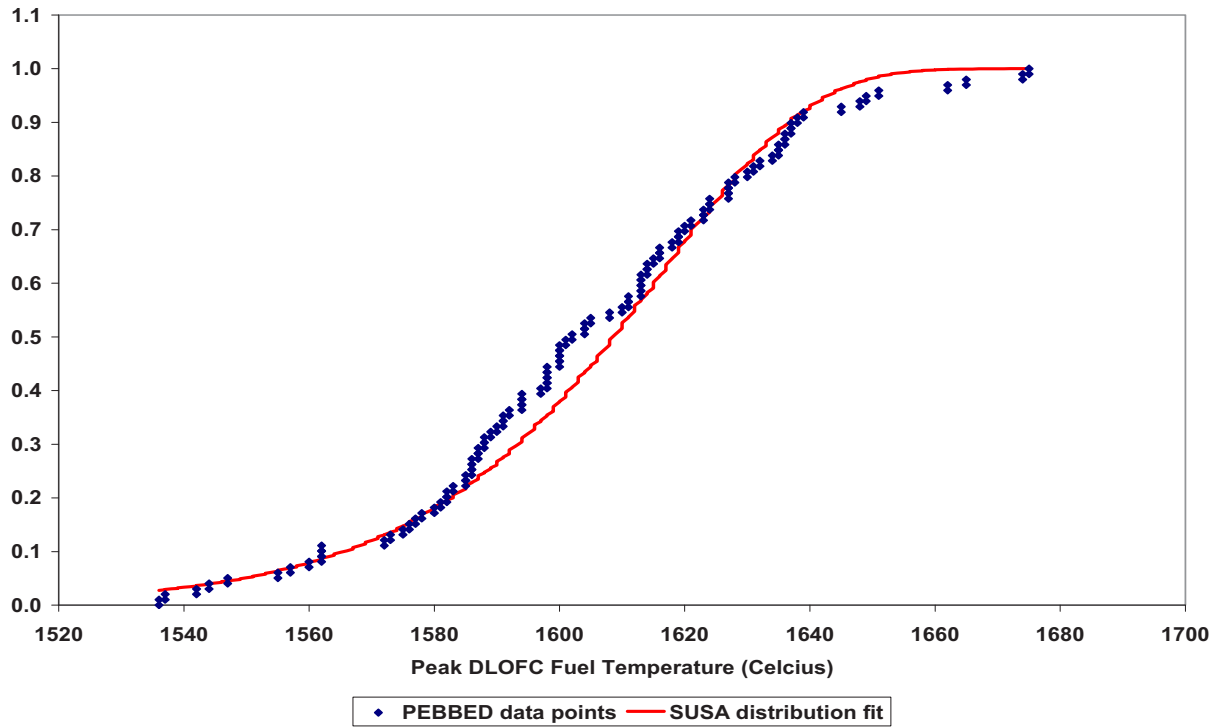


Figure 21. PDF and fitted Weibull distribution results for the 100 LHS Normal set: K-S level of significance = 0.2231.

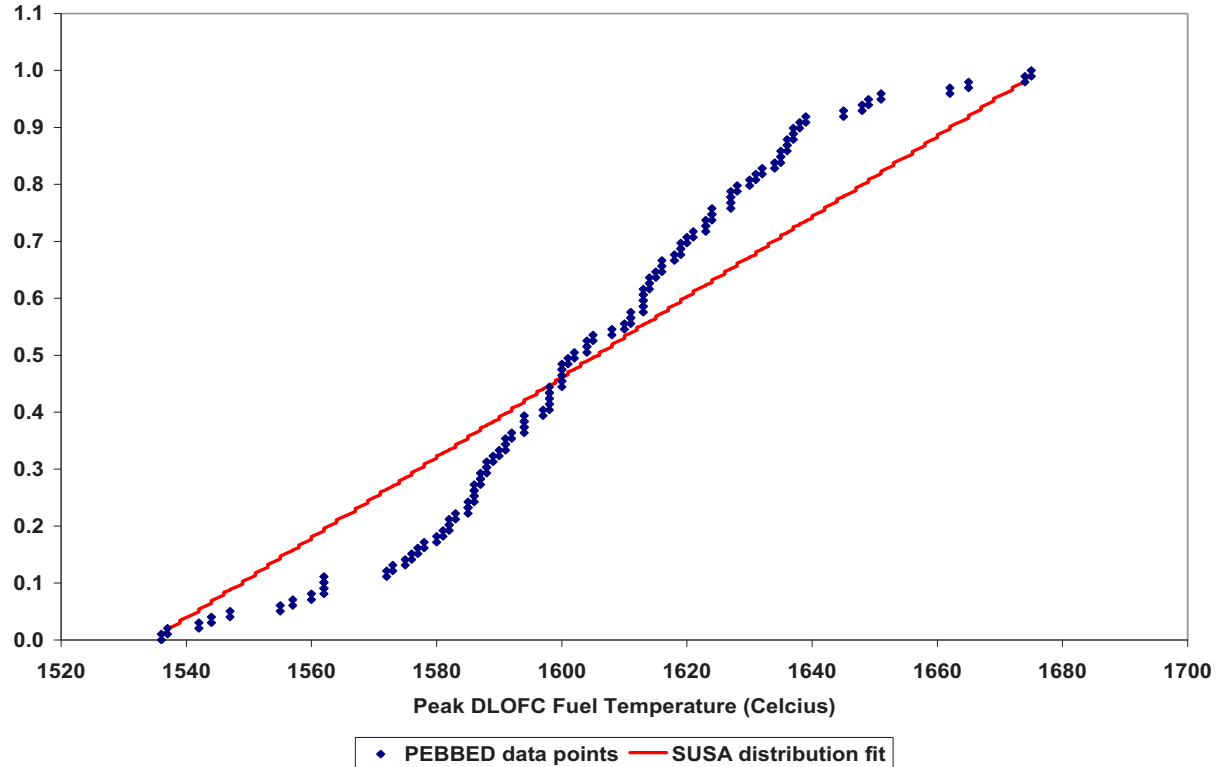


Figure 22. PDF and fitted uniform distribution results for the 100 LHS Normal set: K-S Level of Significance = 0.0026.

A second example of the Lilliefors and K-S test results for the 100 LHS Uniform set is presented in Table 6 and Table 7. Both tests confirm that for this Uniform sampled set, log-normal distribution fits provide the best match for the pebble load rate and the peak fuel temperature.

Table 6. Lilliefors test results for the 200 LHS Normal set.

Figure of Merit	Lilliefors Test: Level of Significance for Distribution Type		
	Normal	Lognormal	Exponential
DLOFC Maximum Fuel Temperature	0.64	0.79	0.01
Pebble Load Rate	0.08	0.1	0.01

Table 7: K-S test results for the 200 LHS Normal set.

Figure of Merit	K-S Test: Level of Significance for Goodness of Fit					
	Normal	Lognormal	Weibull	Uniform	Gamma	Beta
DLOFC Maximum Fuel Temperature	0.924	0.966	0.117	0.002	0.954	0.713
Pebble Load Rate	0.477	0.513	0.019	0	0.502	0.333

A summary of the mean and (95%,95%) two-sided tolerance limits (at the time when the peak fuel temperature are reached) are shown in Table 8 for all six SUSA sets. The actual number of model calculations is also indicated. For three of the sets, one calculation each did not complete successfully, but the remaining 99 and 199 model runs were still an adequate sample size for the statistical analysis. The following observations can be made:

- *Mean values:* The mean values for all six data sets are almost identical (2°C variation on 1604°C, for example), i.e., regardless of the sampling method, parameters included, or distribution types, these six independent random sets predict the same mean DLOFC maximum fuel temperature (1604°C) and pebble load rate (2,793/day).

Table 8: PEBBED CRP-5 DLOFC uncertainty study results.

Number of Model Runs	Input Data			Mean and (95%,95%) Two-Sided Tolerance Limits	
	Input Parameter Sampling Method	Input Parameter Distribution Type	Model Input Parameters Varied	DLOFC Maximum Fuel Temperature (°C)	Pebble Load Rate (Per Day)
99	Latin Hypercube	Uniform	Power, RIT, decay heat only	1,603 ± 61	2,793 ± 72
100	Latin Hypercube	Uniform	Specific heat and thermal conductivity only	1,605 ± 45	2,790*
100	Latin Hypercube	Uniform	All	1,605 ± 76	2,794 ± 72
99	Latin Hypercube	Gaussian/Normal	All	1,604 ± 59	2,793 ± 55
200	Latin Hypercube	Gaussian/Normal	All	1,604 ± 59	2,793 ± 55
199	Simple Random	Gaussian/Normal	All	1,604 ± 58	2,790 ± 57

* No variations in the fuel load rate occurred, since only changes in reactor power result in new fuel load rates.

- *Distribution type:* Using a uniform distribution could be expected to result in the sampling of high and low values more frequently, compared to a normal distribution, since the probability of sampling a high, mean, or low value is identical for a uniform distribution, but there is a lower probability to sample from the low and high tails of the normal distribution. This effect is responsible for the slightly larger uncertainty band ($\pm 76^{\circ}\text{C}$, or 4.7%) for the 100 LHS Uniform set, compared to the 100 and 200 LHS Normal set values ($\pm 59^{\circ}\text{C}$, or 3.7%). The difference is however still minimal: only 17°C on 1604°C .
- *Sampling method:* The mean and (95%,95%) two-sided tolerance limits are identical for the two sets that used the SRS and LHS methods. It does not seem to matter which statistical random generator algorithm is used. This observation is in agreement with the conclusion reached by Helton (2005), where the properties of the SRS and LHS methods were compared and also found to be very similar. This study did, however, recommend using LHS because of its enforced stratification over the sample range, and one participant in the BEMUSE benchmark (De Crécy 2008) pointed out that the SRS approach might not be optimal for sensitivity studies.
- *Number of model calculations:* Model calculations are crucial time-consuming factors for the statistical uncertainty method. This small set (800 model runs is still a relatively small population number in typical statistical analysis – a few 1,000 is typically recommended) did not lead to significant differences between sets consisting of 100 or 200 model runs. As pointed out earlier (Section 3.4, and Figure 16), a low number of runs (10 or 30) will definitely lead to partially populated distributions and erroneous conclusions. The Wilks' formula recommendation (93 calculations) therefore seems to be sufficient for this model and transient. This conclusion is supported by the ATHLET PWR study (Glaeser 2008) where 100 model runs were performed for 56 uncertain input parameters, and most of the participants in the BEMUSE benchmark study (De Crécy 2008) did between 93 and 150 model runs for 13 to 49 input parameters. Four of the BEMUSE benchmark participants found that the 95th percentile can typically be directly obtained from a converged PDF after 400 to 500 model runs, if parallel resources are available, or if the model run times are not significant. The final recommendation was that Wilks' formula should be applied at the third or fourth order (between 124 and 153 model runs).
- *Dominant input factors:* Even before an analytical sensitivity study is performed to determine which of the factors are responsible for most of the variations in the output data, the first two data sets shown here already show that the power, inlet gas temperature, and decay heat variations contribute significantly to the variation seen in the DLOFC peak fuel temperature. On its own, these three small input variations produced an uncertainty band of $\pm 61^{\circ}\text{C}$, while the much larger uncertainty variations in the five material correlations only lead to a value of $\pm 45^{\circ}\text{C}$. Note that both these sets can be compared with the 100 LHS Uniform set where all eight input variables were included, and (95%,95%) two-sided tolerance limits of $\pm 76^{\circ}\text{C}$ were obtained.

A single example of the time dependent nature of the data shown in Table 8 is provided in Figure 23, which shows the data for the 200 LHS Normal set. As indicated earlier, the minima and maxima (which is the upper and lower bounds of the model calculations in Figure 15) vary with time, and the resultant distribution properties show similar variations. The uncertainty bandwidth increases with time beyond the time point where the peak fuel temperature is reached, i.e., in this example the highest fuel temperatures and the largest uncertainty variations do not occur at the same time point.

It has been shown in this section that the input uncertainties in only eight parameters already lead to (95%,95%) two-sided tolerance limits of $\pm 59^{\circ}\text{C}$ (or 3.7%) around the mean value of 1604°C for the peak fuel temperature during a DLOFC transient in the PBMR design. A more complete study, taking into account all known input uncertainties could possibly lead to a larger uncertainty bandwidth. These uncertainties need to be taken into account during the reactor safety margin design process.

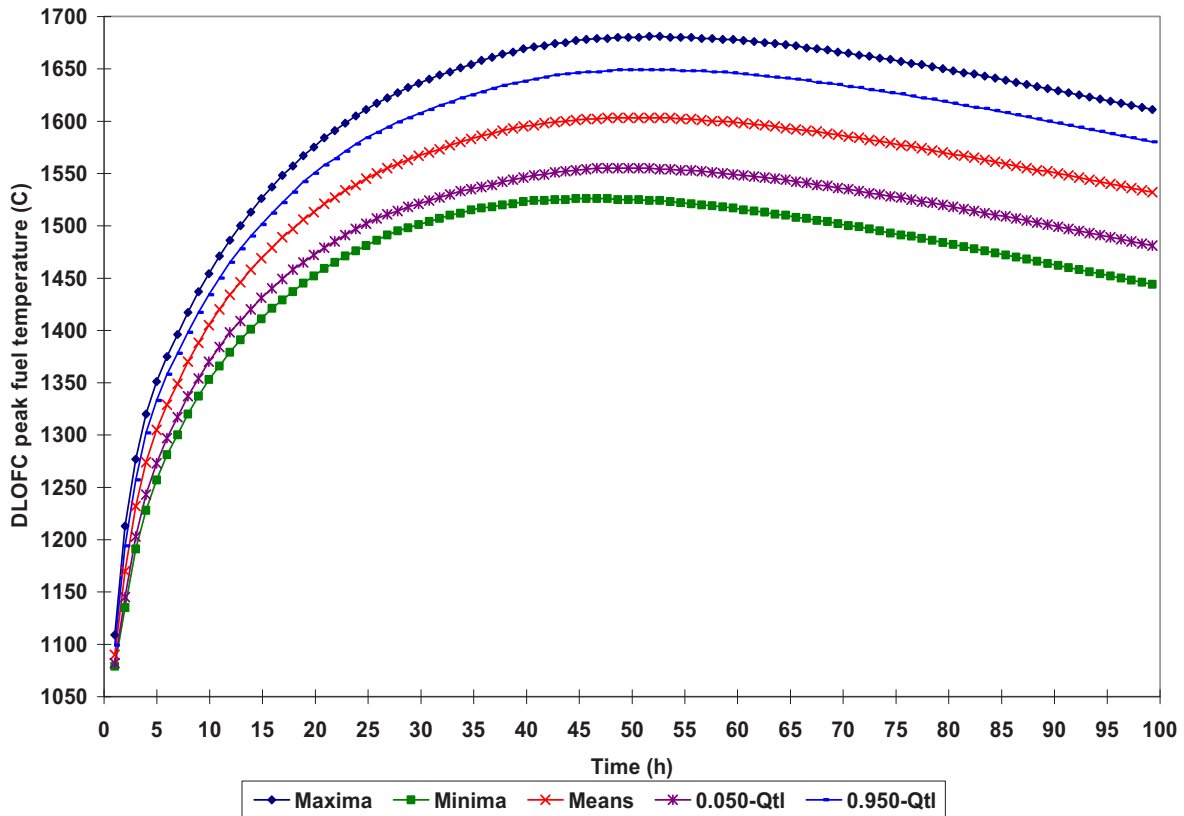


Figure 23. Time dependent minima, maxima, means and 5/95 percentiles for the 200 LHS Normal set maximum fuel temperature.

3.6 Sensitivity Analysis

Selected results of two sensitivity studies are presented in this section: a simple parametric variation of the eight input variables between their minimum and maximum values, and the SUSA analysis of the same six data sets that were produced in Section 4.5.

3.6.1 Parametric Variation Study Results

In the PIRT process, a simple parametric sensitivity study can be performed to aid with the selection of a smaller set of uncertain input parameters. The input parameters are varied one by one in sequential model calculations using their minimum and maximum values in order to isolate their effect on the output parameters of interest. The magnitudes of the variations were obtained from the TINTE study (Strydom 2004), and are identical to the values used in the uncertainty study (Table 3). The results from the simple parametric variation study are presented in Table 9, and can be summarized as follows:

- The ranked entries show that a small variation of $\pm 2\sigma = 5.7\%$ in the decay heat correlation is responsible for the largest change of $\pm 50^\circ\text{C}$ (3.1%) in the DLOFC peak fuel temperature. (Note that the 5.7% uncertainty is prescribed by the DIN standard because of the error in the fitted correlation). This effect is almost twice as large as the second most influential input parameter (pebble bed effective conductivity), which was varied by $\pm 2\sigma = 8\%$.

Table 9: Parametric variation study results.

Input Parameter Varied	$\pm 2\sigma$ Values	Difference between Reference and Varied Cases' Maximum Fuel Temperatures (°C)			
		Steady State		DLOFC	
		- Case	+ Case	- Case	+ Case
Decay heat multiplication factor	0.943 and 1.057	0	0	-50	50
Pebble bed effective conductivity multiplication factor	0.86 and 1.14	0	0	31	-25
Reflector conductivity multiplication factor	0.90 and 1.10	0	0	25	-22
Reactor power	392 and 408 MW	-12	12	-19	19
Fuel specific heat multiplication factor	0.94 and 1.06	0	0	10	-10
Reflector specific heat multiplication factor	0.90 and 1.10	0	0	8	-7
RIT	490 and 510°C	-10	10	-4	4
Fuel conductivity multiplication factor	0.92 and 1.08	5	-3	1	0

- Only three parameters had a non-zero effect on the steady-state fuel temperature: total power, inlet gas temperature, and fuel conductivity. The effect of the uncertainties in these parameters also did not all propagate through to the DLOFC phase—only the total power had a similar or stronger effect during the DLOFC.
- Uncertainties in the measured mass flow rate (shown here as power variations) and inlet gas temperatures (both examples of measurement uncertainties or long-term instrumentation drift errors) have similar levels of influence.
- Uncertainties in the reflector and pebble bed graphite conductivity also produced variations in the DLOFC peak fuel temperature of more than $\pm 1\%$.
- The TINTE and PEBBED sensitivity study results and conclusions are almost identical. The small differences that exist between the TINTE and PEBBED studies are the result of model differences, e.g., the use of virgin graphite versus 36 full-power years.

3.6.2 SUSASensitivity Study Results

This section presents selected results from the SUSASensitivity study. An overview of the definitions, uses, and advantages of typical sensitivity parameters (regression coefficients, correlation measurements, partial and empirical coefficients, etc.) can be found in Helton (2006). As indicated previously, SUSASensitivity can calculate several quantitative measures of correlation between the uncertainties in input parameters and the subsequent variations in the output data. Since the model calculations are usually expensive in terms of computational requirements, it is accepted practice to use the same data sets for the sensitivity and uncertainty analyses. The Kendall rank correlation coefficients and the empirical correlations ratios shown in Figure 24 to Figure 29 can therefore be generated for any of the six data sets used in Section 4.5. (The indexes of the parameters from Nos. 1 to 8 in the figures are: power, inlet temperature, decay heat, fuel specific heat, reflector specific heat, fuel conductivity, bed conductivity, and reflector conductivity, and all data shown here is for their effects on the maximum fuel temperature).

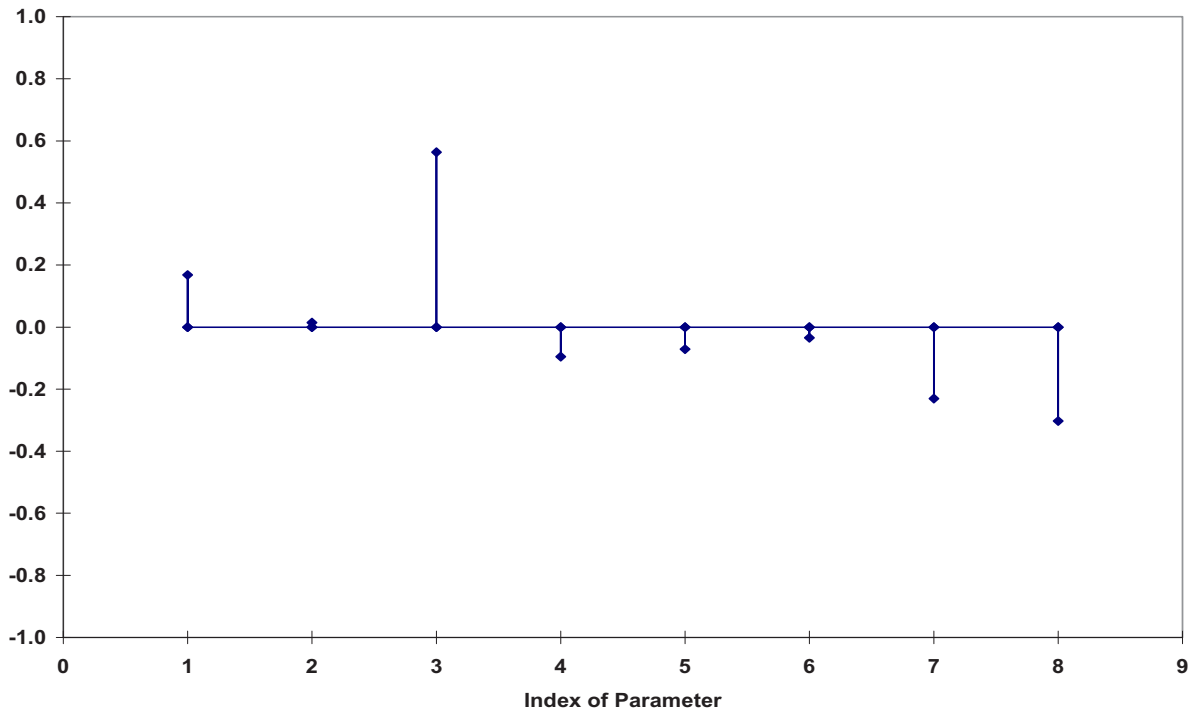


Figure 24. Kendall rank correlation coefficients (peak fuel temperature) for the 100 LHS Uniform set.

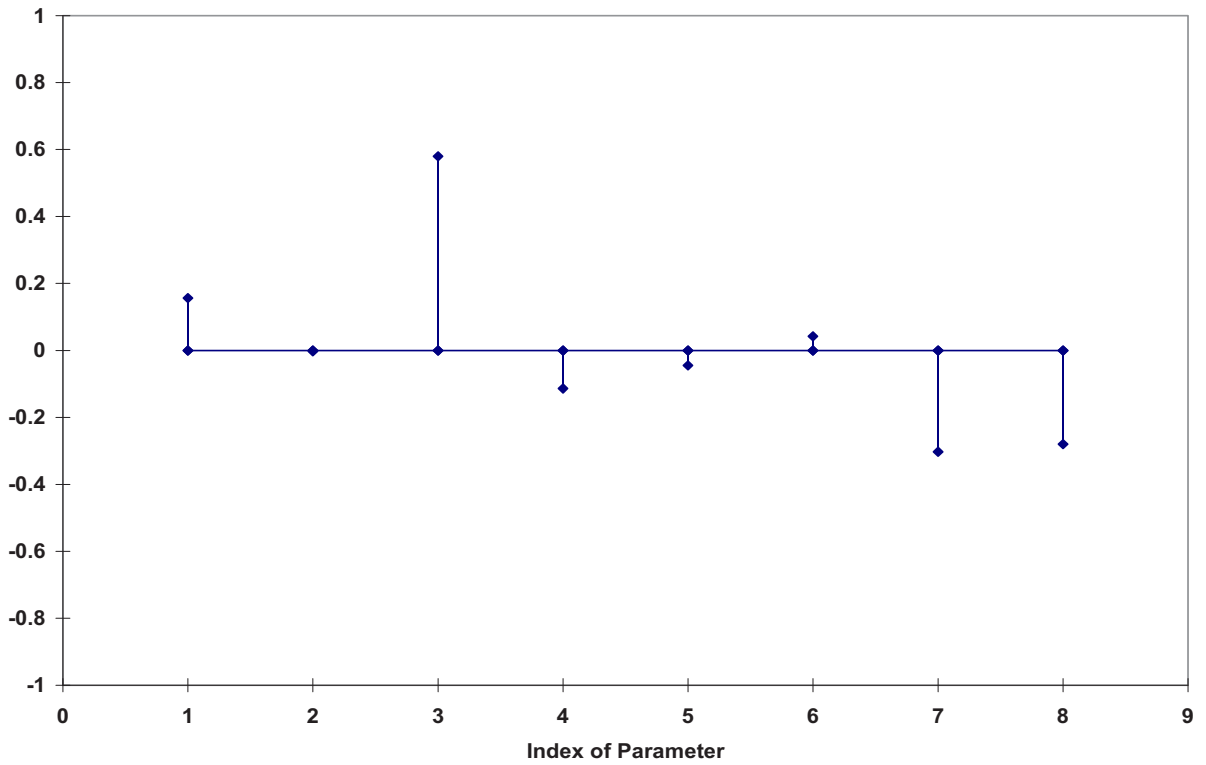


Figure 25. Kendall rank correlation coefficients (peak fuel temperature) for the 200 LHS Normal set.

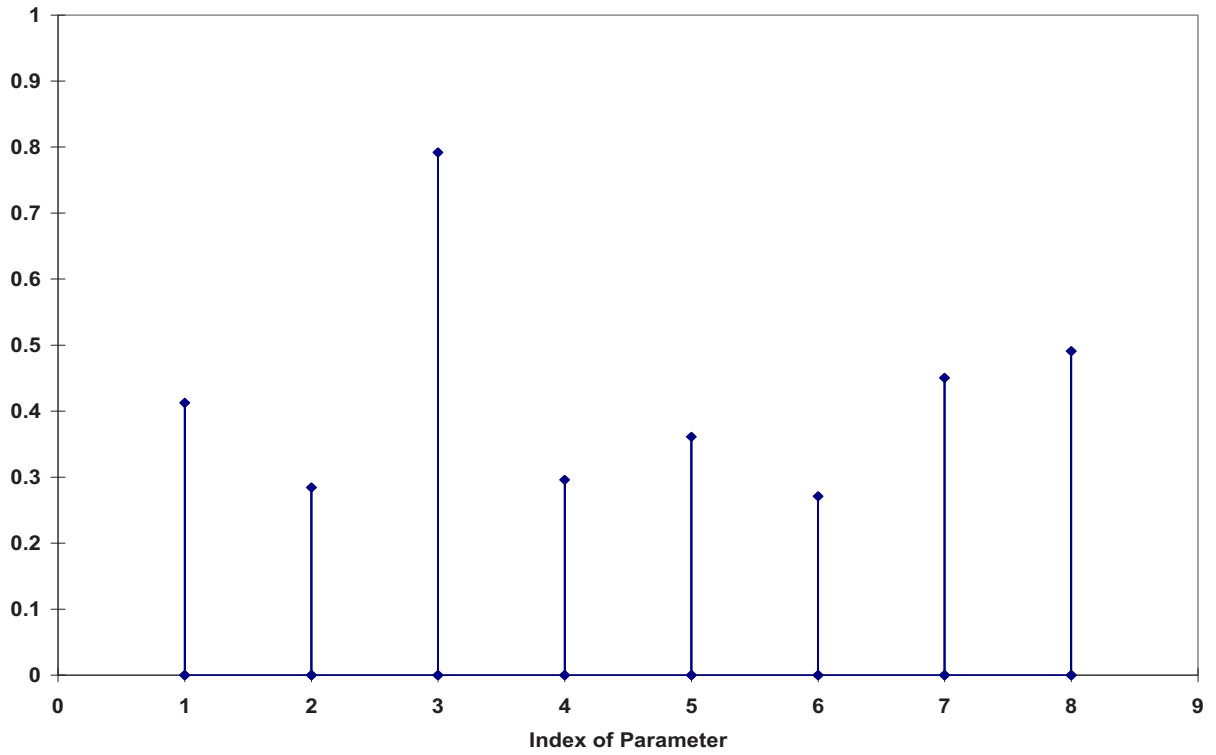


Figure 26. Empirical correlation ratios (peak fuel temperature) for the 100 LHS Uniform set.

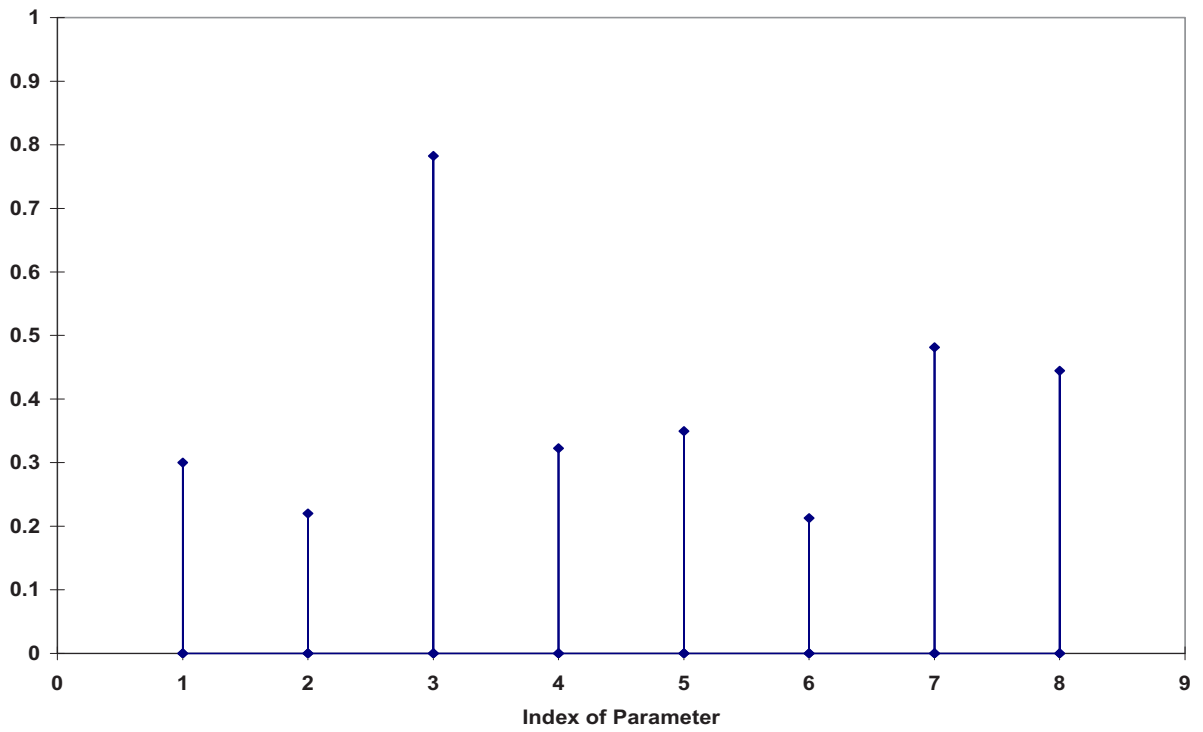


Figure 27. Empirical correlation ratios (peak fuel temperature) for the 200 LHS Normal set.

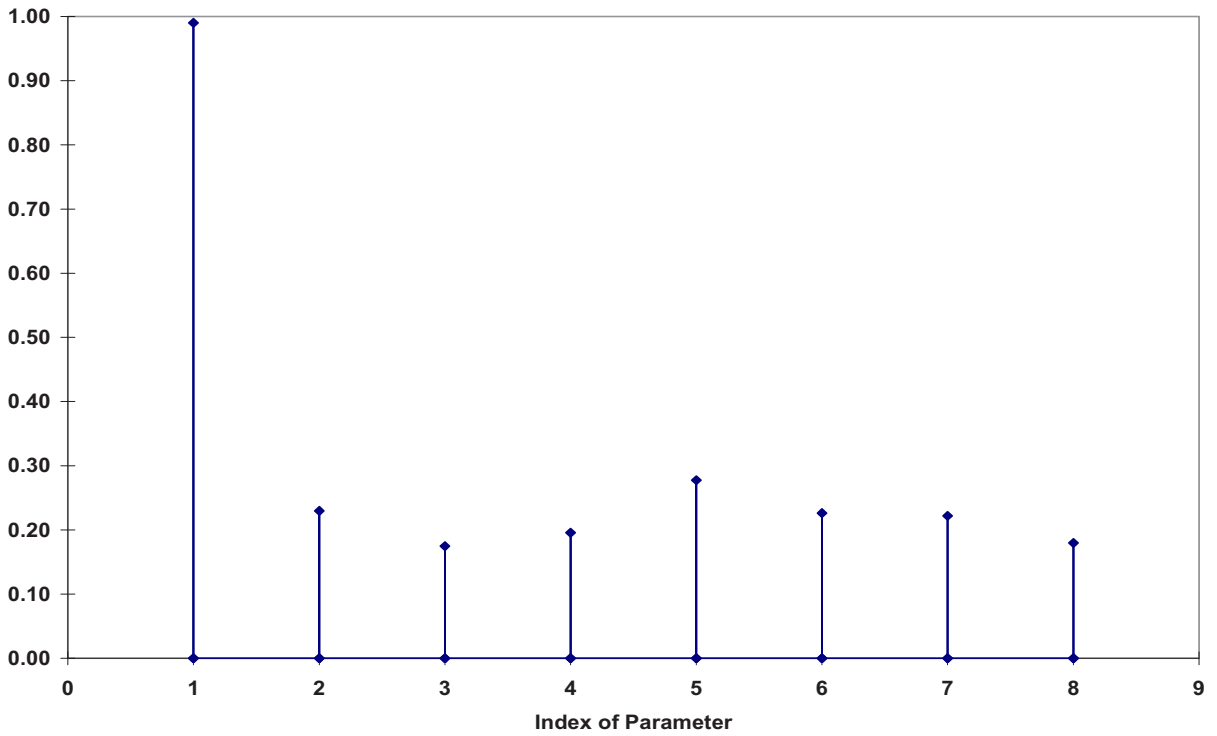


Figure 28. Empirical correlation ratios (pebble load rate) for the 200 LHS Normal set.

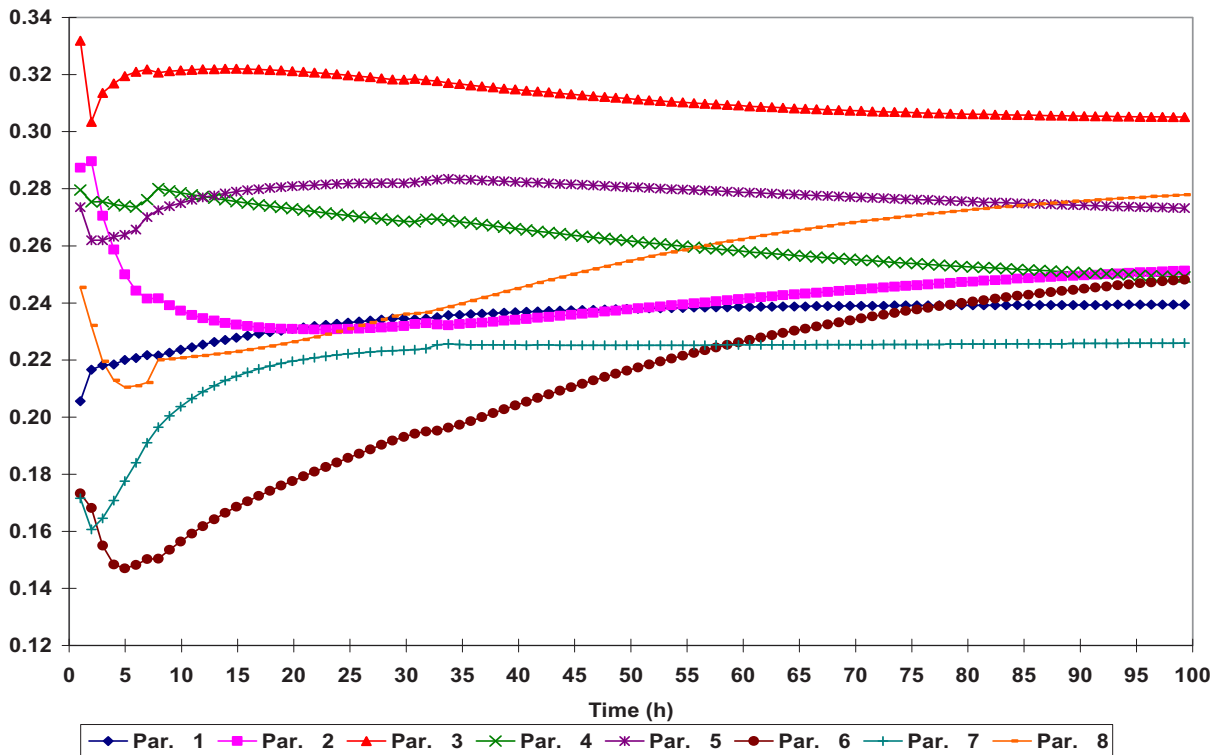


Figure 29. Empirical correlation ratios (peak fuel temperature) variations vs. time for the 200 LHS Normal set.

The *magnitude* of the coefficients provides insight into the degree which a specific input parameter influences the output parameter values (zero values imply almost no link between the input and output uncertainty variations), while the *sign* of the Kendall coefficient indicate a positive or negative relationship (e.g., an increase in decay heat will lead to an increase in fuel temperature). This information can be used to confirm the effect of known physical phenomena or to highlight the primary drivers behind the output uncertainty variations.

Apart from a change in order between input Parameters 7 and 8, the results of the 100 LHS Uniform set shown in Figure 24 and 200 LHS Normal set shown in Figure 25 are very similar. According to the SUSA analysis, the three primary drivers of uncertainty in the fuel temperature are the decay heat and the reflector and pebble bed conductivity. This finding is in agreement with the parametric sensitivity study results (Section 4.6.1), where these three factors were also identified as being responsible for the largest changes in the output fuel temperature.

The empirical correlation ratios shown in Figure 26 and Figure 27 do not show a directional influence (all values are positive), but the three primary drivers can still be readily identified. This indicator is known to be more sensitive to the number of model calculations performed; when the data for the 100 LHS Uniform set shown in Figure 26 and 200 LHS Normal set shown in Figure 27 are compared, it can be seen that the three primary parameters' amplitudes (3, 7, and 8) remained similar, but the values of the lesser contributors decreased for the 200 model calculations set. The need for a higher number of model runs to distinguish low-level contributions in sensitivity studies is also identified in the literature (De Crécy 2008 and Helton 2006), and should be kept in mind when a low number of model runs are used for sensitivity conclusions. (Note that the Wilks criteria on the validity of using a limited number of model runs only applies to uncertainty studies, and cannot be extended to sensitivity studies).

A good example of spurious correlations is shown in Figure 28, where a value of 1.0 is calculated for the empirical correlation ratio of the total power and the pebble load rate, and values of 0.2 to 0.3 for the other seven input parameters. The correlation ratios of Parameters 2 through 8 are noise data caused by the statistical nature of a small sample set, and should, in principle, have had zero values, since the pebble load rate in the PEBBED code can only be influenced by variations in the power.

As a final example, the time dependent empirical correlation ratios for the 200 LHS Normal data set (Figure 29) illustrate the principle that the rank of the input parameters is not constant over time (e.g., compare the correlation ratios at 5 and 100 hours).

4. CONCLUSIONS

This report summarizes the results of the initial investigations performed with SUSA, utilizing a typical high temperature reactor benchmark (the IAEA CRP-5 PBMR 400 MW Exercise 2) and the PEBBED-THERMIX suite of codes. The following steps were performed as part of the uncertainty and sensitivity analysis:

1. Eight PEBBED-THERMIX model input parameters were selected for inclusion in the uncertainty study: the total reactor power, inlet gas temperature, decay heat, and the specific heat capability and thermal conductivity of the fuel, pebble bed, and reflector graphite.
2. The input parameters variations and probability density functions were specified, and a total of 800 PEBBED-THERMIX model calculations were performed, divided into 4 sets of 100 and 2 sets of 200 steady-state and DLOFC transient calculations each.
3. The steady-state and DLOFC maximum fuel temperature and the daily pebble fuel load rate data were supplied to SUSA as model output parameters of interest. The 6 data sets were statistically analyzed to determine the 5 and 95% values for each of the three output parameters with a 95% confidence level, and typical statistical indicators were also generated (e.g., Kendall, Pearson, and Spearman coefficients).
4. A SUSA sensitivity study was performed to obtain correlation data between the input and output parameters, and to identify the primary contributors to the output data uncertainties.

It was found that the uncertainties in the decay heat, pebble bed, and reflector thermal conductivities were responsible for most of the propagated uncertainty in the DLOFC maximum fuel temperature. It was also determined that the two standard deviation (2σ) uncertainty on the maximum fuel temperature was between $\pm 58^{\circ}\text{C}$ (3.6%) and $\pm 76^{\circ}\text{C}$ (4.7%) on a mean value of 1604°C . These values mostly depended on the selection of the distribution types, rather than the number of model calculations above the required Wilks criteria (a (95%,95%) statement would usually require 93 model runs).

Possible future investigations could include the following:

- Clarify the approach on complex non-statistical uncertainties: bypass flows, core thermal dispersion, radial/axial power peaking, Control Rod worths, etc.
- A comparison of the results obtained with SUSA and the Sandia National Laboratory code DAKOTA.
- The propagation of the uncertainties in the cross section data from the basic nuclear ENDF libraries to the PEBBED steady-state represents a longer term challenge. In this regard, promising results have been produced in 2010 with a special version of SUSA developed for this task as part of the UAM benchmark (XSUSA). The implementation of XSUSA at INL's VHTR group is planned for 2011, as part of the forthcoming Prismatic VHTR Benchmark activities.

5. REFERENCES

- 10 CFR 50.46, 1996, "Acceptance Criteria for Emergency Core Cooling Systems for Light Water Nuclear Power Reactors," Appendix K to 10 CFR Part 50: "ECCS Evaluation Models," *Code of Federal Regulations*.
- CR-5249, 1989, "Quantifying Reactor Safety Margins: Application of Code Scaling, Applicability, and Uncertainty Evaluation Methodology to a Large Break Loss of Coolant Accident" (2nd Edition), NUREG/ CR-5249, EG&G Idaho, Inc.
- Ball, S. J., et al., 2007, "Next Generation Nuclear Plant Phenomena Identification and Ranking Tables (PIRTs). Volume 2: Accident and Thermal Fluids Analysis PIRTs," NUREG/CR-6944, Vol. 2.
- Boyack, B. E., et al, 1990, "Quantifying Reactor Safety Margins Part 1: An Overview of the CSAU Evaluation Methodology," *Nuclear Engineering and Design*, Vol. 119, pp.1–15.
- Chakravarti, et al., 1967, *Handbook of Methods of Applied Statistics*, Vol. I, John Wiley and Sons, pp. 392–394.
- D'Auria, F., Giannotti, W., 2000, "Development of Code with Capability of Internal Assessment of Uncertainty," *Journal of Nuclear Technology*, Vol. 131, Issue 1, pp. 159–196.
- De Crécy, A., et al., 2008, "Uncertainty and Sensitivity Analysis of the LOFT L2-5 Test: Results of the BEMUSE Programme," *Nuclear Engineering and Design*, Vol. 238, pp. 3561–3578.
- Glaeser, H., 2008, "GRS Method for Uncertainty and Sensitivity Evaluation of Code Results and Applications," *Science and Technology of Nuclear Installations*, Vol. 2008, Article ID 798901.
- Gougar, H., Yoon, W., Ougouag, A., 2010, "Multiscale Analysis of Pebble Bed Reactors," *Proceedings of HTR 2010*, Prague, Czech Republic.
- Gougar, H. D., et al., 2010, "Automated Design and Optimization of Pebble Bed Reactor Cores," *Nuclear Science and Engineering*, Vol. 165, Nr. 3, pp. 245–269.
- Helton, J.C., et al, 2005, "A comparison of Uncertainty and Sensitivity Analysis Results Obtained with Radom and Latin Hypercube Sampling," *Reliability Engineering and System Safety*, Vol. 89, pp. 305-330.
- Helton, J. C., et al, 2006, "Survey of Sampling-based Methods for Uncertainty and Sensitivity Analysis," *Reliability Engineering and System Safety*, Vol. 91, pp. 1175–1209.
- Hiruta, H., et al., 2008, "CYNOD: A Neutronics Code for Pebble Bed Modular Reactor Coupled Transient Analysis," *Proceedings HTR2008, Washington, D.C., USA*.
- Ivanov, K., et al., 2007, "Benchmark for Uncertainty Analysis in Modeling (UAM) for Design, Operation and Safety Analysis of LWRs: Volume I Version 1.0: Specification and Supporting Data for the Neutronics Cases (Phase I)," NEA/NSC/DOC(2007)23.
- Langebusch, S., et al., 2005, "Comprehensive Uncertainty and Sensitivity Analysis for Coupled Code Calculations of VVER Plant Transients," *Nuclear Engineering and Design*, Vol. 235, pp. 521–540.
- Lilliefors, H., 1967, "On the Kolmogorov-Smirnov Test for Normality with Mean and Variance Unknown," *Journal of the American Statistical Association*, Vol. 62. pp. 399–402.
- Maritz, J.S., 1981, *Distribution-Free Statistical Methods*, Chapman & Hall. ISBN 0-412-15940-6, p. 217.
- McKay, M.D., et al., 1979, "A Comparison of Three Methods for Selecting Values of Input Variables in the Analysis of Output from a Computer Code," *Technometrics* (American Statistical Association), Vol. 21, Issue 2, pp. 239–245.

- Reitsma, F., et al., IAEA-TECDOC, "Evaluation of High Temperature Gas Cooled Reactor Performance Benchmark analysis related to the PBMR, GT-MHR, HTR-10 and the ASTRA Critical Facility," In Preparation.
- Rodgers, J. L., Nicewander, W. A., 1988, "Thirteen Ways to Look at the Correlation Coefficient," *The American Statistician*, Vol. 42, Issue 1, pp. 59–66.
- Salah, A. B., et al., 2006, "Uncertainty and Sensitivity Analyses of the Kozloduy Pump Trip Test Using Coupled Thermal-Hydraulic 3D Kinetics Code," *Nuclear Engineering and Design*, Vol. 236, pp. 1240–1255.
- Strydom, G., 2004, "TINTE Uncertainty Analysis of the Maximum Fuel Temperature during a DLOFC Event for the 400 MW Pebble Bed Modular Reactor," *Proceedings HTR2004, Pittsburgh, USA*.
- Wilks, S. S., 1941, "Determination of Sample Sizes for Setting Tolerance Limits," *Annals of Mathematical Statistics*, Vol. 12, No. 1, pp. 91–96.
- Yates, D. S., et al., 2008, "The Practice of Statistics," 3rd Ed., Freeman Press, ISBN 978-0-7167-7309-2.

APPENDIX A

Summary of Changes Made to the PEBBED and THERMIX Codes for SUSA Implementation

APPENDIX A

Summary of Changes Made to the PEBBED and THERMIX Codes for SUSAN Implementation

Source Code Changes

The SUSAN uncertainty study required a number of minor changes to the THERMIX source code to allow the use of multiplication factors for the decay heat, specific heat and thermal conductivity correlations, as indicated in Table A-1 (no changes were needed for the PEBBED source code). In total less than 200 lines of code were changed. A sequential test approach was followed during the development phase, consisting of:

- Backward compatibility tests to ensure that 0.0 input values in older input decks were converted to multiplier values of 1.0.
- Multiplier input values equal to 1.0 produced identical results compared to the original source.
- Multiplier input values not equal to 0.0 or 1.0 produced physically consistent results, when compared to the TINTE (Time Dependent Neutronics and Temperatures) study (Strydom 2004). This step consisted of simple up and down variations in the multiplier input values (e.g. 0.9 and 1.1), and confirming the direction and magnitude of the changes on the output data.

In addition to these changes, a set of data input and output reading/writing tools were also created using the same Fortran 90 compiler that was used for the compilation of the PEBBED-THERMIX source (Compaq Visual Fortran, version 6.6a). These routines can also easily be integrated in the SUSAN Fortran shell for complete SUSAN control over all aspects of the uncertainty calculations (instead of performing the PEBBED-THERMIX calculations off-line, as was done for this study).

The changes were all performed on a released version of PEBBED-THERMIX dated July 9, 2010, that also included the latest COMBINE 7 upgrades. The THERMIX User Manual will also be revised at a later stage to include a description of these changes.

Table A-1. Summary of THERMIX source code changes.

Subroutine	Line No.	Description
xlamt.f90	10–22, 279–291, 351–356, 543–548, 557–563, 605–611	Use of module SUSAs added. Setting of local variables, and modification of fuel, reflector and pebble bed <i>thermal conductivity</i> formulas to account for addition of multiplication factors.
xlam.f90	9–13, 58–64	Use of module SUSAs added. Setting of local variables for use in xlamt.f90.
wkptkbb.f90	5–14, 22–29, 106–112, 156–160	Use of module SUSAs added. Setting of local variables, and modification of fuel and reflector <i>specific heat</i> formulas to account for addition of multiplication factor.
wkpt.f90	5–14, 23–31, 79–86, 115–121, 164–175	Use of module SUSAs added. Setting of local variables, and modification of fuel and reflector specific heat formulas to account for addition of multiplication factors.
wkap.f90	11–15, 74–79, 123–129	Use of module SUSAs added. Setting of local variables, and modification of <i>fuel specific heat formula</i> to account for addition of multiplication factor.
tproz.f90	12	Use of module SUSAs added.
steuer.f90	11–17, 384–389, 535, 680–685	Use of module SUSAs added. Calls to wkap.f90 and reduz.f90 updated with additional passed variables.
reduz.f90	10, 62, 85–99	Inclusion of global routine tmxglobals.h added. Modification of <i>decay heat</i> formulas to account for addition of multiplication factor.
maithx.f90	50–54, 435–440, 453–459	Use of module SUSAs added. Call to xlam.f90 updated with additional passed variables.
konst1.f90	96–101	Call to xlam.f90 updated with additional passed variables.
ein11.f90	10–14, 228–240, 653–691, 839–844	Use of module SUSAs added. Read & write format of input card TX11 modified to include multiplication factors for <i>fuel and reflector specific heat</i> , as well as <i>reflector, fuel and bed thermal conductivities</i> , as entries on positions #4–9. Call to wkptkbb.f90 updated with additional passed variables.
calt2h.f90	12–16	Use of module SUSAs added.
caltah.f90	12–16	Use of module SUSAs added.
writetmxldofc.f90	172–177	Read & write format of input card TX3 modified to include “decay_mod” factor as entry on position #11.
susa.f90	1–16	New module that contains commonly used variables names and definitions.

Input File Changes

The power and inlet gas temperature input specifications were not modified, since these parameters were already part of the required input data for PEBBED and THERMIX. The five correlation multiplication factors for the decay heat, specific heat and thermal conductivities were therefore the only new additions to the THERMIX input file (the PEBBED file required no changes), as listed in Table A-2. Note that backwards compatibility was achieved by setting missing or zero values to the default multiplier value of 1.0.

Table A-2. Summary of THERMIX input file changes.

Card	Entry No. on card	Variable name	Value and Description
TX3	11	decay_mod	>1.0: Decay heat multiplication factor. <=0.0: Zero value modified to default value of 1.0.
TX11	4	c_fuel_mod	>1.0: Fuel graphite specific heat multiplication factor, implemented for material function number 17 and a constant value. <=0.0: Zero value modified to default value of 1.0.
TX11	5	c_refl_mod	>1.0: Reflector graphite specific heat multiplication factor, implemented for material function numbers 7, 13, 14 and 15 and a constant value. <=0.0: Zero value modified to default value of 1.0.
TX11	6	cond_refl_mod	>1.0: Reflector thermal conductivity multiplication factor, implemented for material function number 3 and a constant value. <=0.0: Zero value modified to default value of 1.0.
TX11	7	cond_fuel_mod	>1.0: Fuel thermal conductivity multiplication factor, implemented for material function numbers 2, 7 and 24 and a constant value. <=0.0: Zero value modified to default value of 1.0.
TX11	8	cond_bed_mod	>1.0: Effective pebble bed thermal conductivity multiplication factor, implemented for material function numbers 25-27 and a constant value. <=0.0: Zero value modified to default value of 1.0.